https://ntrs.nasa.gov/search.jsp?R=19680028256 2020-03-12T05:38:05+00:00Z

USCEE 304

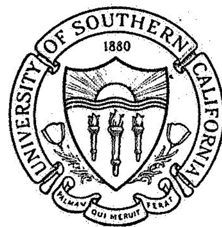

Final Report

Period from 1 July 1967 - 30 September 1968

UNIVERSITY OF SOUTHERN CALIFORNIA

LOCALIZED VIBRATIONAL MODES OF LITHIUM AND LITHIUM-DEFECT PAIRS IN SILICON

Principal Investigator: William G. Spitzer

Sponsored by the
.tional Aeronautics and Space Administration
Under Grant 05-018-083

GPO PRICE $
CFSTI PRICE(S) $
Hard copy (HC)
Microfiche (MF)
ff 653 July 65

:CTRONIC SCIENCES LABORATORY

N68-37728
(ACCESSION NUMBER)
(THRU)
72
(PAGES)
1
(CODE)
CR-97309
(NASA CR OR TMX OR AD NUMBER)
26
(CATEGORY)
FACILITY FORM 602

USCEE 304

Final Report

Period from 1 July 1967 - 30 September 1968

LOCALIZED VIBRATIONAL MODES OF LITHIUM AND LITHIUM-DEFECT PAIRS IN SILICON

Principal Investigator: William G. Spitzer

Sponsored by the
National Aeronautics and Space Administration
Under Grant 05-018-083

Departments of Materials Science and
Electrical Engineering
Division of Electrical Sciences
University of Southern California
Los Angeles, California

TABLE OF CONTENTS

Page

Introduction 1

I. Localized Vibrational Mode of Lithium Diffused, Undoped Silicon 4

A. Review of Local Mode Concepts 4

B. Absorption in the Defect Lattice 8

C. Localized Modes in Boron-Lithium Doped Silicon 10

D. The Isolated, Interstitial Li Vibrational Mode 12

II. Preliminary Experiments in the Infrared Absorption of Electron Irradiated, Lithium Diffused Silicon 16

A. Introduction 16

B. Experimental Method 18

C. Results and Discussion 19

III. Localized Vibrational Mode Absorption of Lithium and Phosphorus Impurities in Germanium 28

IV. Lithium-Boron Defect Pairs in $Si_{1-x}Ge_x$ Alloys 34

V. Localized Vibrational Modes of Substitutional Defect Pairs in Silicon and Lithium Induced Donor Precipitation 36

A. Introduction 36

B. Experimental Method 37

C. Experimental Results 38

1. Localized Mode Frequencies 38

2. Dependence of Absorption Band Intensities on Li Diffusion Conditions 39

D. Discussion of Results 40

1. Localized Mode Frequencies 40

2. Impurity Precipitation Effects 43

VI. Theoretical Calculations of One-and Two-Phonon Optical Absorption from Boron Impurities in Silicon 47

INTRODUCTION

It is the objective of this report to present a description of the work carried out between 1 July 1967 and 30 September 1968 under NASA Research Grant No. 05-018-083.

There are a number of studies which were pursued under this contract, and it will be necessary to divide the main text into several sections which are listed as follows:

(I) Localized Vibrational Mode of Lithium Diffused, Undoped Silicon

(II) Preliminary Experiments in the Infrared Absorption of Electron Irradiated, Lithium Diffused Silicon

(III) Localized Vibrational Mode Absorption of Lithium and Phosphorus Impurities in Germanium

(IV) Lithium-Boron Defect Pairs in $Si_{1-x}Ge_x$ Alloys

(V) Localized Vibrational Modes of Substitutional Defect Pairs in Silicon and Lithium Induced Donor Precipitation

(VI) Theoretical Calculations of One- and Two-Phonon Optical Absorption from Boron Impurities in Silicon

In some cases the results of the investigation have been published, and hence in these cases, the review given here will be quite brief. In those cases where the results have not been published or do not warrant publication, more extensive discussions will be given. In general, we have attempted to make each section somewhat independent of the others to

facilitate readers who may be interested in only one of the topics.

The following personnel were actively engaged in the research reported here:

Faculty: (1) William G. Spitzer

(2) Maurice H. L. Pryce (summer 1967)

Post Doctoral Research Fellow:

L. Bellomonte (left October 1967)

Students: (1) A. E. Cosand

(2) G. Cumming

(3) J. Kung

Publications and papers presented at technical meetings which had their origin in the work to be discussed in this report are listed as follows:

1. Localized Vibrational Modes of Li and P Impurities in Germanium by A. E. Cosand and W. G. Spitzer, Appl. Phys. Letters 11, 279 (1967).

2. Localized Vibrational Modes of Defect Pairs in Silicon by V. Tsvetov, W. Allred, and W. G. Spitzer, Oral presentation to Conference on Localized Excitation Phenomena, Univ. of California at Irvine, September, 1967; Published in Proceedings of Conference on Localized Excitations in Solids, Plenum Press.

3. Calculation of the Optical Absorption Due to Localized Mode-Lattice Vibration Combination Bands in Boron-Doped Silicon by L. Bellomonte and M.H.L. Pryce, Oral presentation to Conference on Localized Excitation Phenomena, Univ. of California at Irvine, September 1967; Published in Proceedings of Conference on Localized Excitation Phenomena, Plenum Press.

4. Calculation of One- and Two-Phonon Optical Absorption from Boron Impurities in Silicon by L. Bellomonte and M.H.L. Pryce, Proc. Phys. Soc. (London), to be published.

5. Vibrational Modes of Boron-Lithium Doped Silicon-Germanium Alloys by A. E. Cosand and W. G. Spitzer presented at American Physical Society Meeting, Berkeley, California, March 1968.

I. Localized Vibrational Mode of Lihtium Diffused, Undoped Silicon

It was one of the first tasks of the present investigation to determine whether there is an observable localized vibrational mode due to isolated interstitial lithium, hereafter called Li_i. In short, we were unable to observe such a localized mode. The possible reasons for our inability to observe the mode require some discussion. However, it is desirable to precede this discussion with somewhat more general sections concerning the nature of localized vibrational mode absorption and application to the case for boron-lithium pair defects in silicon.

A. Review of Local Mode Concepts

In the subject of infrared lattice absorption we usually deal with the lattice dynamics of pure semiconductor crystals, and the interaction between the radiation field and the phonon spectrum of the material. In the present case, however, we are interested in the same subject,but the crystals considered may have large concentrations of defects. It is of particular interest to consider the influence of the defects on the vibrational spectrum and the role the defects play in influencing the absorption of electromagnetic radiation. In almost all cases the imperfections considered are point defects and they are in concentration low compared to atomic concentrations of the host material. It should be clearly understood that we consider here only defect-induced vibrational absorption. We do not consider other types of defect-related absorption such as free carrier absorption and electronic photoexcitation or photoionization of the center.

Defects can cause very substantial changes in the absorption of a semiconductor. They can cause homopolar materials such as silicon to become absorbing as a result of single phonon-photon processes which are forbidden in the perfect crystal. Defects can cause very sharp absorption bands to appear at frequencies well above the maximum phonon frequency or in the gap between the optical and acoustical parts of the phonon spectrum of the unperturbed lattice. The only lattice absorption processes which occur in this frequency range in the crystal with no defects are those related to interaction between the radiation and two or more phonons, i.e., multiphonon absorption. If the proper conditions are met, it is also possible for absorption bands to be introduced within the range of allowed phonon frequencies.

The subject of defect induced absorption has been extended both theoretically and experimentally in recent years, and it has given considerable information not only about the vibrational properties of the system but also about the defects themselves.

The space lattice of the diamond structure is the cubic close packed (fcc) and the atomic sites associated with each space lattice point (p, q, r) are at (p, q, r) and ($p + a/4$, $q + a/4$, $r + a/4$) where a is the lattice constant. Thus the crystal structure is one of two interlocking face centered cubic lattices, and the atoms are all tetrahedrally bounded. There is a center of inversion midway between nearest neighbors. This is the crystal structure of both Si and Ge.

The primitive cell of the face centered cubic lattice is trigonal, and there are two atoms per cell. Thus there are 6 branches to the phonon vs. wavevector ($\vec{q}$) curves, 3 of which are optical and 3 acoustical. In Si and Ge, the inversion symmetry leads to a degeneracy of the LO (longitudinal optical) and LA (longitudinal acoustical) branches at the zone edge in the $< 100 >$ direction. The degeneracy is lifted in the zincblend structure. Both of the transverse branches are doubly degenerate for the special directions in $\vec{q}$ space.

The maximum phonon energy, the LO branch near $\vec{q} = 0$ in Fig. I-1*, is generally $\omega_m \lesssim 0.1$ eV for the materials of interest. Therefore, for processes involving the absorption of a photon with the creation of a phonon, conservation of energy requires the photon be in the infrared. Conservation of wave vector means that only phonons near $\vec{q} \sim 0$ can be involved, and the necessity of coupling between the radiation field and the phonons leads to an interaction only with the TO branches. The coupling is through the dipole moment of the TO mode. Thus single-photon-phonon absorption can occur in the III-V compounds but is symmetry forbidden in Si and Ge. It is this absorption which accounts for the well-known residual ray behavior of polar and partially polar crystals and is often known as the fundamental lattice absorption.

Processes involving the absorption of a photon with the creation of two or more phonons (multiphonon summation absorption) occurs in Si and Ge. In this case also the conservation of wave vector applies and means that the two phonons must have nearly equal and opposite $\vec{q}$ values (or the

---

*Each figure, table and reference in this report is labelled by a Roman numeral representing the particular section and by an Arabic numeral representing the sequence within the section.

same values for difference absorption where one phonon is created and the photon with another phonon is absorbed). Density of states arguments lead to the conclusion that most of the phonons involved are in several relatively small frequency ranges. These frequencies originate from regions near the zone edges where the phonon branches have small slopes in $\vec{q}$ space. Thus the multiphonon absorption is often analyzed in terms of combinations of a few frequencies which are called characteristic frequencies. More sophisticated analysis interprets the changes in slope of the absorption in terms of two phonon critical points, i.e., regions where the ω vs q of the sum or difference of two branches has zero slope in $\vec{q}$ space.

The coupling in the multiphonon case is either via absorption by the fundamental which then decays into two phonons through anharmonicity in the potential or through a second order electric moment mechanism. The first process requires an optically active fundamental and is therefore inoperative in Si and Ge. For a more detailed discussion of all of these points the reader is referred to two recent review papers[I-1, I-2].

The theory of the effect of defects on the normal modes and eigenfrequencies of a lattice have been discussed extensively by several authors. The contributions of A. Maradudin[I-3, I-4, I-5] and R. Elliott[I-6, I-7, I-8, I-9] are particularly well known.

Some of the essential features can be introduced from physical reasoning by considering an isotopic, substitutional defect in a Si lattice. The isotopic assumption means that the defect atom has a mass M' which

may differ from that of Si but the force constants remain unchanged from the Si-Si values. If the defect atom were extremely light compared to Si then we would expect a mode in which the impurity is vibrating against an almost stationary lattice. This mode would have a frequency ω_L considering higher than the highest phonon frequency of the unperturbed system ω_m. In this case the light impurity's high natural resonance frequency $\omega_L \propto \sqrt{\frac{k}{M'}}$ makes M' acts as a high frequency driving force on the neighboring lattice. The lattice is being driven at a frequency well above its highest unperturbed normal mode frequency and thus the amplitude of motion is exponentially attenuated as a function of distance from M'. Since the site of M' has T_d point group symmetry, the potential for small displacements of M' is that of a spherical harmonic oscillator, and thus the high frequency mode is triply degenerate. As the mass of M' is increased we expect the local mode frequency ω_L to decrease and approach ω_m. At the same time the attenuation length should increase. This high frequency mode is often called a "localized mode" because of the spatial localization.

B. Absorption in the Defect Lattice

Infrared absorption by vibrations of defects in Si was treated by Dawber and Elliott[I-6, I-7] for both the local mode and the band modes. The model used was that of a substitutional, charged impurity in a homopolar lattice and the result for the localized mode is

$$\alpha(\omega) = \frac{2\pi^2 De^2}{nc} \left|\chi(o)\right|^2 g(\omega)$$

where

$g(\omega)$ is line shape function normalized to unity by

$$\int_0^\infty g(\omega)\, d\omega = 1$$

$\alpha(\omega)$ is the linear absorption coefficient at the frequency ω
n is the refractive index

D is the defect concentration

$|\chi(o)|^2$ is a correction factor to account for the fact that not all of the vibrational energy is carried by the defect which is located at the origin.

The quantity $|\chi(o)|^2 M' \to 1$ for an arbitrarily light defect. Dawber and Elliott have also calculated the "band mode" absorption and found

$$\alpha(\omega) = \frac{2\pi^2 D e^2}{3\, nc} |\chi(f, o)|^2 S(\omega)$$

where

$S(\omega)$ is the density of states function and

$|\chi(f, o)|^2$ is the quantity corresponding to $|\chi(o)|^2$ in the local mode equation except it now carries the mode label, f.

Note that there is no selection rule on q and all band modes may absorb.

The calculations have been applied to a number of cases of substitutional impurities in Si.

An interesting sum rule for the absorption exists and is

$$\int_0^\infty \alpha(\omega)\, d\omega = \frac{2\pi^2 e^2 D}{ncM'} ,$$

where the integration includes both local and band mode absorption. It may also be noted that for the local mode alone

$$\int_0^\infty \alpha(\omega)\, d\omega = \frac{2\pi^2 De^2}{nc} \int |\chi(o)|^2 g(\omega)\, d\omega$$

which in the limit of small M' becomes the same as the right side of the preceding equation. Therefore, for very light defects the absorption is largely in the local mode.

Some recent work of Leigh and Szigeti [I-10, I-11] has indicated that the quantitative conclusions of the above are questionable in that the polarization effects are important. These authors show that because of the electrostatic field of the impurity, the motion of the uncharged host atoms may result in a contribution to the dipole moment of a mode. Moreover, there may be nearest neighbor or short range forces which may have important effects on the absorption. Because of these difficulties much of the discussion of the experimental intensity observation will be qualitative in nature.

C. Localized Modes in Boron-Lithium Doped Silicon

Localized vibrational modes have been known for many years in semiconductors primarily by the famous oxygen bands in silicon and germanium. However, our present interest is primarily in the boron-

lithium system in silicon.

A number of groups have studied boron doped silicon(I-12, I-13, I-14) which is compensated by Li. The Li diffused interstitially in silicon and is a shallow state donor. Low temperature photoionization and photoexcitation studies(I-15) indicate that Li_i^+ is in a site of T_d symmetry. In pure Si the solid solubility of Li near room temperature(I-16) is $\sim 10^{14} cm^{-3}$. However, studies have shown(I-17) that in p-type material the hole concentration raises the solid solubility of $Li_i^+ + e^-$ until near compensation is achieved. It is found that p-type Si with a room temperature resistivity $\rho_{RT} \sim 10^{-2} \Omega$ cm, when diffused with Li at temperatures in excess of $\sim 550^{\circ}C$, can become $\rho_{RT} > 10^3 \Omega$ cm. It is also known from mobility and diffusion studies(I-17) that much of the Li_i^+ exists in an ion paired state with the B_{Si}^-, ionized substitutional boron acceptor. Thus it is to be expected that the local mode spectrum will become complicated.

Examples of absorption spectra for B-Li doped Si are given in Fig. I-2. The qualitative explanation(I-18, I-19) for the observed effects is based on ion pairing. The Li_i^+ is assumed to be in a nearest neighbor interstitial position to the B_{Si}^- which is in any of four equivalent < 111 > directions from the B site. The modes therefore become those of the pair $B_{Si}^- - Li_i^+$ with point group symmetry C_{3v}. Waldner et. al. (I-19) assumed that the B-Li force constant was small compared to the B-Si and Li-Si force constants. This model predicts the independence of the 655 and 564 cm^{-1} bands on Li isotope as a result of these modes being almost completely B modes. The higher frequency one is double degenerate, the lower one non-degenerate. If the splitting of the B triply degenerate mode by the Li is assumed to be primarily via electrostatic interaction, the observed frequency splitting is in reasonable agreement with the nearest neighbor spacing. There should be a similar effect on the triply degenerate mode of isolated Li_i^+, however, only one Li

mode is observed at 522 cm^{-1} for ^{7}Li or 534 cm^{-1} for ^{6}Li. It is assumed that this band is the high frequency member of a pair where the other band falls below $\omega_{max}(q) \sim 520$ cm^{-1}. Thus a low frequency local mode band will not be observed.

It has been suggested(I-31) that the 522 cm^{-1} band may be related to the presence of Li-O complex formation. Since the 522 cm^{-1} band occurs when no other Li-O or O bands are observed in Si, since the band has been observed in float zone low [O] silicon with a strength equal to that in pulled crystals, and since the band strength is directly proportional to [B], the Li-O complex explanation is unlikely.

Elliott and Pfeuty(I-9) have applied their theory to the B-Li pair case and conclude that they can make a reasonable fit the observed spectra if the force constant for the B-Si bond is lowered along the Li-B direction. Bellomonte and Pryce(I-20, I-21) have calculated the ω_L frequency of isolated interstitial Li as a preliminary step to the study of the effect of pairs. They find that isolated Li may also have a local mode although it is pointed out that the numerical values obtained in the calculation cannot be regarded as very accurate.

D. The Isolated, Interstiaial Li Virbrational Mode

From the preceding discussion it is clear that the interpretation of the 522 cm^{-1} absorption band is that it is the high frequency, doubly degenerate Li_i^+ mode for $(B_{Si}^- - Li_i^+)$ defects. Since ω_m, the maximum phonon frequency of the pure silicon, is at ~ 520 cm^{-1}, we are forced to conclude that the isolated Li_i^+ will not have a high frequency localized mode. However, since the calculations of Bellomonte and Pryce conclude that the Li_i might have a local mode, we decided to look carefully in the spectral region from

$450\ cm^{-1}$ to $\sim 800\ cm^{-1}$. There are several difficulties with this measurement. Since the Li_i^+ is a shallow donor it will be nearly fully ionized at room temperature. With the lithium concentration $[Li_i^+] \simeq n_e = 4 \times 10^{17} cm^{-3}$, the free carrier absorption coefficient at $\omega = 500\ cm^{-1}$ is $\alpha \simeq 150\ cm^{-1}$ yielding a free carrier absorption cross section $\alpha / n_e = 37 \times 10^{17} cm^2$. From the measurements at lower temperatures where the carrier are repopulating the donor levels, the absorption cross section for donor photoionization is of the same order as that for free carriers. Thus the absorption does not drop at lower temperatures. From the (B-Li) pair absorption at $\omega = 522\ cm^{-1}$ we estimate the local mode cross section to be $\sim \frac{\alpha(522)}{[Li]} = 0.05 \times 10^{-17} cm^2$. Therefore, the local mode absorption cross section may be approximately three orders of magnitude less than that for free carriers at $\omega \sim 500\ cm^{-1}$. While it is true that the frequency dependence of the free carrier absorption is of the ω^{-2} form, we have to go near $\omega \sim 1500\ cm^{-1}$ before the carrier cross section drops one order of magnitude. Thus we can see that the local mode band will probably be in a region of very high background absorption making observation difficult.

As indicated previously, our attempts to observe the Li_i^+ mode were not successful. Samples were diffused with lithium to yield carrier concentrations $n_e \gtrsim 5 \times 10^{17} cm^{-3}$. Measurements were made with scale expansions such that $\alpha_{band}/\alpha \sim 5 \times 10^{-3}$ for a band halfwidth of $\sim 4\ cm^{-1}$ should have been observable. Measurements were also made comparing a Li doped sample with one doped with arsenic and close to the same n_e. Again, no absorption band in the Li doped sample was observed. We must conclude that there is no evidence from these measurements for the existence of the isolated Li_i^+ vibrational mode. A disappointing but not unexpected result.

REFERENCES

I-1. W. G. Spitzer, Semiconductor and Semimetals, Vol. 3, (Edited by R. K. Willardson and A. C. Beer, Academic Press, New York, 1967), p. 17.

I-2. F. A. Johnson, Progress in Semiconductors, Vol. 9, (Pergamon Press, Oxford, 1965).

I-3. A. A. Maradudin, Solid State Physics, Vol. 18 (Edited by F. Seitz and D. Turnbull, Academic Press, New York, 1966).

I-4. A. A. Maradudin, Solid State Physics, Vol. 19 (Edited by F. Seitz and D. Turnbull, Academic Press, New York, 1967).

I-5. A. A. Maradudin, E. W. Montroll, G. H. Weise, Solid State Physics, Suppl. 3 (Edited by F. Seitz and D. Turnbull, Academic Press, New York, 1963).

I-6. P. G. Dawber and R. J. Elliott, Proc. Phys. Soc. 81, 453 (1963).

I-7. P. G. Dawber and R. J. Elliott, Proc. Roy. Soc. 273, 222 (1963).

I-8. R. J. Elliott, Lectures on Defects in Solids, Lectures at Argonne National Laboratory; available as ANL-7237 from Clearinghouse for Federal Scientific and Technical Information NBS, U. S. Department of Commerce, Springfield, Virginia.

I-9. R. J. Elliott and P. Pfeuty, J. Phys. Chem. Sol. 28, 1627 (1967).

I-10. R. Marshall and S. S. Mitra, Phys. Rev. 134, A1019 (1964).

I-11. R. S. Leigh and B. Szigeti, Proc. Roy. Soc. A301, 211 (1967).

I-12. J. W. Corbett, G. D. Watkins, and R. S. McDonald, J. Phys. Chem. Sol. 25, 873 (1964).

I-13. W. Kaiser and C. D. Thurmond, J. Appl. Phys. 30, 427 (1959).

I-14. W. Nazareiwicz and M. Balkanski, J. Phys. Chem. Sol. 25, 437 (1964).

I-15. J. F. Angress, A. R. Goodwin, and S. D. Smith, Proc. Roy. Soc. A287, 64 (1965).

I-16. W. G. Spitzer and M. Waldner, J. Appl. Phys. 36, 2450 (1965).

I-17. For references see M. Hass, Semiconductors and Semimetals, Vol. 3 (Academic Press, New York, 1967).

I-18. R. M. Chrenko, R. S. McDonald, and E. M. Pell, Phys. Rev. 138, A1775 (1965).

I-19. R. L. Aggarwal, P. Fisher, V. Mourzine, A. K. Ramdas, Phys. Rev. 138, A882 (1965).

I-20. L. Bellomonte and M. H. L. Pryce, Proc. Phys. Soc. 89, 967 (1966).

I-21. L. Bellomonte and M. H. L. Pryce, Proc. Phys. 89, 973 (1966).

II. Preliminary Experiments in the Infrared Absorption of Electron Irradiated, Lithium Diffused Silicon

A. Introduction

The previous section described the difficulties in the attempts to measure the isolated Li_i^+ mode. The present section describes some preliminary attempts to observe the localized modes of Li_i^+ paired with either a vacancy or a divacancy. For this reason samples were diffused with Li, electron irradiated, and then taken through isochronal anneals between room temperature and 600°C. These experiments are similar to a more extensive set of measurements reported by Prof. John C. Corelli in NASA Grant NGR-33-018-090, Progress Report: 15 June 1967 to 15 March 1968. However, as we were in contact with Prof. Corelli and because the requirements of our experiments are somewhat different, the experimental conditions are not the same as those employed by him.

Reasonably pure, low oxygen content silicon was diffused with Li under conditions to obtain the maximum $[Li_i^+]$ we could produce. However, under these conditions, the $[Li] >> [Li_i^+]$. Some samples were irradiated by 1.8 Mev electrons with a fluence of 1-2 x 10^{18} e/cm^2 and these samples were compared with the unirradiated ones. The large $[Li_i^+]$ was used to enhance the probability of $(Li_i^+ - V_{Si})_{pair}$ formation.

While the experimental details will be discussed shortly, the principal results may be listed as follows:

1) For the samples of [Li] $\simeq 10^{19}$ cm^{-3}, there is a large tail on the absorption edge. The origin of this tail is probably scattering from precipitated Li.

2) The low frequency absorption which is presumably due to free carriers, decreases with increasing anneal temperature up to $\sim 200^{o}$-300°C, then increases with higher anneal temperature. Long term anneal (24 hours) at 600°C removes most free carrier absorption. This behavior is qualitatively explicable in terms of the temperature dependencies of the solid solubility and diffisuion constant for Li. The arguments do not depend in any essential way upon the irradiation produced defects.

3) After annealing at $\sim 450^{o}$C, both the irradiated and unirradiated samples had a strong broad absorption band which peaks near 2μ, close to but not the same as the 1.8 μ divacancy band. The band anneals out by 600°C and is present only in the samples of high [Li]. The origin of this band is not understood.

4) No $(Li_i^+ - V_{Si})_{pair}$ absorption band was observed. However, as a result of these measurements, experiments can be proposed which should enhance the prospects of observing such a band.

B. Experimental Method

The silicon used in this study was ordered from Wacker Chem. Co. It is floating zone (FZ) silicon (low oxygen content) with resistivity greater than 10 ohm-cm. The 2cm diameter silicon ingot was sliced into 1.5mm thick wafers by a diamond saw, and those wafers were further cut into 7mm x 15mm x 1.5mm pieces by a wire saw.

The diffusion of lithium (Li) into silicon was conducted in two steps. First was to alloy lithium on the surface. Lithium mineral oil paste was painted on the surface of sample and then heated in an inert gas until it formed an alloy layer. The second step was to diffuse the lithium into the sample. A vertical furnace was preheated to $1000^{\circ}C$ and flushed with inert gas. The alloyed sample was burried with silicon carbide powder in a tantalum boat. The container and sample were heated in the furnace at $1000^{\circ}C$ for a desired period of time (~ hrs) and then quenched by dropping into mineral oil.

Four of our samples treated in the above manner were electron irradiated. Irradiation was done by a 1.8 Mev Van de Graaff at Aerospace Corporation.* The sample temperature was maintained at $100^{\circ}K$ by contact with a liquid nitrogen bath. The radiation rate was $\sim 1.1 \times 10^{14}$ electron/sec -cm^3. The total dosage was $\sim$ 1-2 x 10^{18} electron/cm^2. These samples are called 1R. 2R. 3R and 4R.

All the annealing steps for both irradiated and unirradiated samples were done in an inert gas unless otherwise specified. Even in the inert gas, the sample surface sometimes gets a stained appearance, especially when annealed at higher temperatures. In this case, we used Linde 0.3A Micron Abrasive on silk to repolish the surface.

Two Perkin-Elmer infrared grating spectrometers were used to measure the absorption spectra; the Model 210 and Model 301. With Model 210 the sample was held in a metal dewar with CsI windows. When measured with Model 301 the sample was fastened on a sample holder plate; sometimes a beam condenser

* We thank Dr. E. J. Stoffel and Mr. L. Rachal for letting us use the radiation facilities.

was employed when the sample has been broken and thus reduced in size. The condition of measurements and annealing procedures are listed in Table II-1.

C. Results and Discussion

The results are plotted in Fig. II-1 through Fig. II-8. All curves in these figures are specified by the same coding as in the "RUN" column in Table II-1. Fig. II-1 shows the transmission spectra in the long wave length region of an unirradiated sample. Fig. II-2 and Fig. II-3 show the transmission spectra of two irradiated samples, 1R and 2R respectively. Note that sample IR was measured at liquid nitrogen temperature. Most of the curves for sample 2R shown in Fig. II-3 were measured at 20°C except the unannealed one which was measured at liquid nitrogen temperature. Measurements of sample 3R are not shown in the figures as they showed nearly the same behavior as 2R. Fig. II-4a and Fig. II-4b show the room temperature absorption spectra at different annealing stages of irradiated sample 4R. Liquid nitrogen measurements of sample 4R at the same annealing stages showed no distinct difference compared with the general behavior of the room temperature measurements. The room temperature absorption spectra of an unirradiated sample 5B are shown in Fig. II-5a and Fig. II-5b. For the same reason as in sample 4R, the results of liquid nitrogen measurements are not shown in this report. Fig. II-6 shows the transmission spectra of sample PFL-1. The preparation of these samples will be stated later.

All the samples except PFL-1 showed a reverse annealing phenomenon at around 200° ~ 300°C. This can be seen on both irradiated and unirradiated samples. (Fig. II-1 through Fig. II-5b). The PFL-1 sample was cut from the same ingot as the other samples but lithium diffused at Goddard Space Flight Center by Dr. Paul Fang's group*. The diffusion temperature was low (~ 500°C) and no fast quenching was employed. All the other samples were diffused at our

*We thank Mr. Walter Wappous for preparing the sample for us.

laboratory by using higher temperature ($\sim 1000^{o}C$) for more than three hours and fast quenched to room temperature. From Fig. II-9 the solid solubility of lithium(II-6) in silicon at $1000^{o}C$ ($\sim 6 \times 10^{19} cm^{-3}$) is much greater than that at $500^{o}C$ ($\sim 4 \times 10^{18} cm^{-3}$). Due to fast quenching there should be more lithium in this sample. But from measurements, both samples showed well within the same order of magnitude for the free carrier concentration, $\sim 4 - 6 \times 10^{17} cm^{-3}$. This suggests that there is a large amount of precipitated lithium particularly in the high temperature, quenched samples. The reverse annealing phenomenon can be explained by considering the presence of precipitated lithium. From Fig. II-9 we notice that the solid solubility of lithium at $27^{o}C$ is $\sim 2 \times 10^{13} cm^{-3}$, while the $n = 4\text{-}6 \times 10^{17} cm^{-3}$ from free carrier absorption measurement. The sample is not in thermal equilibrium. As the temperature of the sample is raised, we expect a more rapid approach toward equilibrium. Thus part of the lithium will get out of the solid solution (either to the precipitate sites, or to the surface of the sample) at lower temperature annealing stages (below $200^{o}C$). Due to the low temperature and short annealing period, the sample can not reach thermal equilibrium; but nevertheless the concentration of free carriers is reduced, thus we observed the decrease of absorption. (Fig. II-4a, Fig. II-5a). At temperatures between $200^{o}C \sim 300^{o}C$, close to the thermal equilibrium state can be reached (compare the small deviation between curves 2R-2 and 2R-3 annealed at $200^{o}C$/40 min and $200^{o}C$/24 hrs. respectively, in Fig. II-3). The lithium solubility is around $5 \times 10^{16} cm^{-3}$ at this annealing stage. Thus we observed a very low absorption. For a higher annealing temperature the solubility of lithium is higher thus lithium will dissolve back into silicon from the precipates. Thus the free carrier concentration goes up and we observed an increase of absorption. (curve 4R-8a in Fig. II-4a and curve 5b-8a in Fig. II-5a). At all the annealing stages, the sample surface always served as a lithium sink. Up to around $500^{o}C$, the out diffused lithium can be replenished from the lithium precipitation. But for

higher temperature annealing ($\gtrsim 550^{o}C$), the solubility of lithium is very high ($> 6 \times 10^{18} cm^{-3}$), all the lithium precipitation may be used up, but the out diffusion process will not stop. As a result, the lithium concentration will again decline, thus a decrease of absorption is observed. (Fig. II-4b, curve 4R-11a, Fig. II-5b, curve 5b-11a). When annealed at $600^{o}C$ for 24 hours, most of the lithium will be out diffused, thus the sample was nearly transparent. (Fig. II-8). During the annealing process some of the curves showed very little frequency dependence of the absorption at low frequency. While this absorption is tentatively ascribed to intraband free carrier transitions, it is recognized that the predicted free carrier absorption $\propto \nu^{-p}$ (where $1.5 \lesssim p \lesssim 3$) is not observed. (For instance curves 5b-1a, 5b-9 in Fig. II-5b). Further investigation is necessary here.

We also observed an absorption band near $2.0\,\mu$ after the $450^{o}C$/30 min. annealing. The band remained during the next two annealing stages, namely $500^{o}C$/30 min and $550^{o}C$/30 min. It disappeared completely after $600^{o}C$/24 hour annealing (Fig. II-8). We observed this band on both the electron irradiated sample 4R(Fig. II-4b) and the unirradiated sample 5b (Fig. II-5b). Sample PFL-1 also went through the same annealing steps as did on the 5b and 4R, but without showing any absorption band near $2.0\,\mu$. (Fig. II-6).

A $1.8\,\mu$ absorption band is well known as an electronic transition in irradiated silicon.[II-1, II-2, II-3, II-4, II-7] Cheng et al[II-4] attributed this band to divacancy absorption. All the observations indicated in the reference were made on non-lithium diffused silicon and the $1.8\,\mu$ absorption band annealed completely between $100^{o}C$ to $200^{o}C$ for neutron irradiated sample or at a temperature below $350^{o}C$ for electron irradiated sample[II-8]. To our knowledge, no one has ever observed a $1.8\,\mu$ band in non-irradiated silicon.

A quantitative measurement of the $2.0\,\mu$ absorption band is difficult because the high frequency dependent background. In the electron irradiated sample the background is in itself due to a radiation produced band which was called "the absorption edge band" by Fan and Ramdas[II-3]. In a lithium precipitated silicon

sample the background appears to follow an $\sim\lambda^{-2}$ relationship. Similar behavior was observed in neutron-irradiated GaAs. Calculation of the infrared absorption for a distribution of small metallic inhomogeneities in an otherwise uniform nonmetallic crystal was carried out and obtained excellent agreement[(II-5)] with the λ^{-2} region of neutron irradiated GaAs. For the above reason, only a qualitative analysis of the 2.0 μ band is possible.

Three absorption bands with background substracted are plotted in Fig. II-7. They were from measurements (c.f. Table II-1) 4R-11b (as curve A), 5B-11b (as curve b), and from the paper by Fan and Ramdas[(II-3)] (as curve C), respectively. From Fig. II-7, we notice that curves A and B are shifted to the lower wave number side of the spectrum and are far broader than curve C. A comparison between curves A and B shows that they have the same width and centered at about the same frequency. The only difference is that curve A is higher (i.e., more absorption) than curve B. At present time, it is not clear yet whether the irradiation made the absorption of curve A larger. Further investigation is needed.

Fig. II-8 shows the transmission spectra of both irradiated sample 4R and unirradiated sample 5B after 600°C annealing. The 2.0 μ band disappeared after a 600°C/30 min. annealing on sample 4R, but a heavy free carrier absorption in the long wave length region was observed, (Fig. II-8, curve 4R-12a). Sample 5b also showed a similar heavy free carrier absorption after a 600°/30 min annealing, in addition a very small absorption band near 2.0 μ was observed, (Fig. II-8, curve 5B-12). A prolonged annealing (24 hrs.) at 600°C in atmosphere was made on both samples, the results showed that both of them were nearly transparent. (Fig. II-8, curves 4R-13, 5B-13).

From the contrast showed in Fig. II-7 together with the low temperature (compare to 450°C) annealing out effect of the divacancy associated 1.8 μ band, it is suggested that the 2.0 μ band we observe may be due to divacancy lithium

complex and is probably a new band. The suggested explanation may be stated as follows: The high annealing temperatures of the suggested trimer, the divacancy $+Li_i^+$, as compared to the divacancy ($600^\circ C$ vs $\sim 350^\circ C$) could arise from the contribution of the pairing energy between the divacancy and the Li_i^+ to the free energy. The source of divacancies could be from either (Li_i^+-vacancy) which are not observed or from the regions near the precipitated Li. Further investigation and detail calculation are necessary to verify this.

REFERENCES

II-1. Becker, Fan and Lork-Horovitz, Phys. Rev. 85, 730(A) (1952).

II-2. M. Nisenoff (unpublished measurement).

II-3. H. Y. Fan and A. K. Ramdas, JAP 30, No. 8, 1127 (1959).

II-4. L. J. Cheng, J. C. Corelli, J. W. Corbett, and G. D. Watkins, Phys. Rev. 152, 761, (1966).

II-5. L. W. Aukerman, Semiconductors and Semimetals, Vol. 4., p. 401.

II-6. E. M. Pell, Solid State Physics in Electronics and Telecommunications, Vol. 1, Part 1, p. 263.

II-7. H. Y. Fan and A. K. Ramdas, J. Phys. Chem. Solids 8, 272 (1959).

II-8. J. C. Corelli, Progress Report, Covering Period from 15 June 1967 to 15 March 1968, Sponsored by NASA, Under Grant NGR-33-018-090.

TABLE II-1

Sample	Lithium Diffusion	Irradiation	Run	Annealing Temp/ Time	Measurement*	Sample Thickness (cm)	Data Plot In Report	Remark
1A	$1000^{o}C$/3 hrs. -$1100^{o}C$/30 min quenched to R. T.	None	1A-1	None	CONT/RT	0.0356	No	
			1A-2	$200^{o}C$/24 hrs.			Yes	
			1A-3	$400^{o}C$/6 hrs.				
			1A-4	$500^{o}C$/6 hrs.				
1R	$1000^{o}C$/3 hrs. quenched to R. T.	1.8 Mev Rate: $1.1\times10^{14}\frac{el.}{sec.\,cm^{3}}$ Temp. $100^{o}K$ Total dose = $1\text{-}2\times10^{18}\frac{el.}{cm^{2}}$	1R-1	None	CONT/LNT	0.0457	Yes	
			1R-2	$200^{o}C$/40 min.		0.0381		
			1R-3	$400^{o}C$/40 min.				
			1R-4	$500^{o}C$/35 min.				
			1R-5	$600^{o}C$/35 min.				
2R	Same as 1R	Same as 1R	2R-1	None	CONT/LNT	0.01956	Yes	
			2R-2	$200^{o}C$/40 min.	CONT/RT	0.02057		
			2R-3	$200^{o}C$/24 hrs.		0.02032		
			2R-4	$300^{o}C$/40 min.				
			2R-5	$350^{o}C$/40 min.				
			2R-6	$400^{o}C$/40 min.				
3R	Same as 1R	Same as 1R	3R-1	None	CONT/RT	0.03556	No	
			3R-2	$200^{o}C$/40 min.				
			3R-3	$400^{o}C$/40 min.				
4R	Same as 1R	Same as 1R	4R-1a	None	PTP/RT	0.047	Yes	
			4R-1b		PTP/LNT		No	
			4R-2a	$90^{o}C$/30 min.	PTP/RT		Yes	
			4R-2b		PTP/ LNT		No	
			4R-3	$150^{o}C$/30min.	PTP/RT		No	

4R	Same as 1R	Same as 1R	4R-4a	$200^oC/30$ min.	PTP/RT		Yes	
			4R-4b		PTP/LNT		No	
			4R-5a	$250^oC/30$ min.	PTP/RT		Yes	
			4R-5b		PTP/LNT		No	
			4R-6a	$300^oC/30$ min.	PTP/RT		Yes	
			4R-6b		PTP/LNT		No	
			4R-7a	$350^oC/30$ min	PTP/RT	0.047	No	
			4R-7b		PTP/LNT		No	
			4R-8a	$400^oC/30$ min	PTP/RT		Yes	
			4R-8b		PTP/LNT		No	
			4R-9a	$450^oC/30$ min	PTP/RT		Yes	
			4R-9b		PTP/LNT		No	
			4R-10a	$500^oC/30$ min.	PTP/RT		Yes	
			4R-10b		PTP/LNT		No	Annealing at 600^oC/24 hrs. was held in atmosphere. Sample was broken during the polishing process before run 4R-13.
			4R-11a	$550^oC/30$ min.	PTP/RT		Yes	
			4R-11b		PTP/LNT		No	
			4R-12a	$600^oC/30$ min.	PTP/RT		Yes	
			4R-12b		PTP/LNT		No	
			4R-13	$600^oC/24$ hrs.	PTP/RT		Yes	
5B	$1000^oC/3$ hrs. quenched to RT	None	5B-1a	None	PTP/RT		Yes	
			5B-1b		PTP/LNT	0.062	No	
			5B-2	$90^oC/30$ min.	PTP/RT		Yes	
			5B-3a	$150^oC/30$ min.	PTP/RT		No	
			5B-3b		PTP/LNT		No	

5B	$1000^{\circ}C$/3 hrs. quenched to R. T.	None	5B-4	$200^{\circ}C$/30 min.	PTP/RT	0.062	Yes	
			5B-5	$250^{\circ}C$/30 min.	PTP/RT		No	
			5B-6a	$300^{\circ}C$/30 min.	PTP/RT		No	
			5B-6b		PTP/LNT		No	
			5B-7	$350^{\circ}C$/30 min.	PTP/RT		No	
			5B-8a	$400^{\circ}C$/30 min.	PTP/RT		Yes	
			5B-8b		PTP/LNT		No	
			5B-9	$450^{\circ}C$/30 min.	PTP/RT		Yes	
			5B-10a	$500^{\circ}C$/30 min.	PTP/RT		Yes	
			5B-10b		CONT/LNT		No	
			5B-11a	$550^{\circ}C$/30 min.	PTP/RT		Yes	
			5B-11b		CONT/LNT		Yes	
			5B-12	$600^{\circ}C$/30 min.	PTP/RT		Yes	5B-13 was annealed in atmosphere
			5B-13	$600^{\circ}C$/24 hrs.	PTP/RT		Yes	
PFL-1	Diffusion of Li was done by Dr. P. Fang's group at Goddard Space Flight Center. Diffusion Temp. was below $500^{\circ}C$. and no quenching process was employed	None	P-1	None	PTP/RT	0.0534	Yes	
			P-2	$90^{\circ}C$/30 min.				
			P-3	$150^{\circ}C$/30 min.	No measurement was made on these steps			
			P-4	$200^{\circ}C$/30 min				
			P-5	$250^{\circ}C$/30 min.				
			P-6	$300^{\circ}C$/30 min.				
			P-7	$350^{\circ}C$/30 min.				
			P-8	$400^{\circ}C$/30 min.	PTP/RT		Yes	
			P-9	$450^{\circ}C$/30 min.			No	
PFL-1			P-10	$500^{\circ}C$/30 min.			Yes	
			P-11	$550^{\circ}C$/30 min.			No	
			P-12	$600^{\circ}C$/30 min.		0.0528	Yes	

*Abbreviation symbols = CONT - continuous measurement;
PTP - point to point measurement;
RT - room temperature measurement;
LNT - liquid nitrogen temperature measurement.

III. Localized Vibrational Mode Absorption of Lithium and Phosphorus Impurities in Germanium

Localized vibrational modes of light impurities in a crystal lattice have been observed by infrared absorption measurements in a large group of crystals including several semiconductors. Among the semiconductors studied are Si, GaAs, GaSb, InSb, CdS, ZnSe.[III-1] It is surprising, therefore, that in Ge no absorption via localized modes had been reported. This material is of particular interest since it is one of the more promising cases where comparison between detailed theoretical calculations and experiment might be made. The only reported fundamental mode transition $\Delta n = 1$, for an impurity in Ge is the recent Raman work of Feldman, et al., for Si-doped Ge.[III-2] In the present work we report infrared absorption measurements of both Li and P high-frequency localized modes in Ge.

Because the impurities used in this study are shallow-state electrical dopants, it is necessary to electrically compensate the sample for the absorption coefficient $\alpha \sim 2\ cm^{-1}$.[III-3] In Ge (single doped to that level we anticipate a similar absorption band strength), however, α (free carrier) is of the order of 10^2 to $10^4\ cm^{-1}$ in the spectral range of interest, $\nu \sim 300$ to $1000\ cm^{-1}$.

The compensation of p-type, B-doped Si by Li diffusion to a point where α (local modes) > α (free carriers) is successful for $p \lesssim 5 \times 10^{20}\ cm^{-3}$.[III-4] However, in Ge for $p \gtrsim 10^{18} cm^{-3}$ the Li compensation is not sufficient to meet the above condition for α.

Thus, for Ge, double doping and a method of crystal growth that gives good homogeneity of doping are required. Samples were therefore grown by the Czochralski method in a < 311 > direction. Phosphorus and Ga are a suitable pair of dopants; they have similar segregation coefficients and high solubilities. Only the P is expected to give rise to a localized mode with $\nu_L > \nu_1$, where ν_L and ν_1 are the local mode and highest unperturbed phonon frequencies, respectively.

The initial material was grown with GaP as the dopant so that in the crystal $[P] \lesssim [Ga] = 3\text{-}4 \times 10^{18}$ cm^{-3}. It was a p-type with $\rho = 20\text{-}40 \times 10^{-3}$ Ω-cm. The material was compensated by diffusing lithium from a surface alloy layer at 500-550°C for 15-25 hr. and then quenching to room temperature within a few seconds to avoid precipitating the lithium.(III-5) The best samples were uniformly n-type immediately after quenching but became high resistivity p-type after a few hours to a few days at room temperature. They were then stored in liquid nitrogen to prevent further change. Care was taken not to heat the samples during grinding and polishing. In none of the samples was it possible to entirely get rid of all background absorption.

In the spectral region from 270 cm^{-1} to 510 cm^{-1} four absorption bands not present in high-purity Ge are found in Li-compensated Ga and P-doped Ge at 80°K (sample 1, Fig.III-1).Two of the bands, at 356 cm^{-1}, and 380 cm^{-1}, change frequency to 379 cm^{-1}, and 405 cm^{-1} if ^{6}Li is used instead of natural Li (93% ^{7}Li). These two bands also appear at the same

frequency in Ga-doped Ge which has been nearly compensated with As and Sb and then diffused with Li (samples 2 and 3, Fig. III-1); the two bands in the Ga- and P-doped material at 343 and 350 cm^{-1} which do not show a Li isotope shift do not appear in this material.

The presence of two Li bands implies that the interstitial Li is in a paired configuration, probably as Li-Ga pairs. The stronger band should then correspond to a doubly degenerate transverse mode and the weaker band to a singly degenerate axial mode. The model used for B-Li pairs in Si[III-6], that of completely localized B and Li vibrations interacting with a simple Coulomb field, predicts the doubly degenerate vibrations to be the higher frequency ones. In Si, the B vibrations qualitatively fitted this model but only one Li mode with ν_L close to ν_1 was observed. In the present case, although ν_L values for both Li modes $> \nu_1$, the ν_L (doubly degenerate) $< \nu_L$ (singly degenerate) and the splitting $\Delta\nu_L$ is much smaller than that predicted by the Coulomb model.

It is not obvious that there should be two P bands as there is only one abundant P isotope. Another specimen was prepared with about twice the doping level of the first P- and Ga-doped specimen. The larger band at 343 cm^{-1} almost doubled in strength from α = 23 cm^{-1} to 39 cm^{-1} while the smaller band at 351 cm^{-1} more than tripled from α = 5 cm^{-1} to α = 16 cm^{-1} (measured in terms of peak absorption strength).

A possible model is that the stronger band is attributed to the triply degenerate mode of isolated substitutional P and the weaker one is

due to P-Ga pairs. It is not unreasonable that only a single additonal band be seen from pairs.

Tsvetov, et al.(III-7) have observed pairing of B with P, As, and Sb in silicon; in each case two additional bands were observed, but in one case, B-P pairs, one of the bands appeared only as a small shoulder on the band due to isolated B while the other band was split off by a substantial amount. If the observed additional band in Ge were the doubly degenerate (and thus stronger) band, a weaker band could well be hidden under the isolated P band.

Elliott and Pfeuty(III-8) calculated the frequencies of local modes of B in Si paired with an impurity of arbitrary mass. For the arbitrary impurity slightly lighter than the host lattice, the situation analogous to P-Ga pairs in Ge, their calculation predicts, for changed mass only with no change in force constants, that the doubly degenerate local mode is at very nearly the same frequency as is that of the isolated lighter impurity of the pair, and the singly degenerate mode is raised in frequency. However, comparison with the experimental results in Si show that force constant changes are not negligible; in the case of B-As pairs in Si the doubly degenerate band is predicted to be at a higher frequency but the stronger of the two bands observed is the lower frequency one.

The phonon spectra for Ge and Si are sufficiently similar when normalized to the same maximum frequency that the calculation by Dawber and Elliott(III-9) for the frequency of local modes in Si should apply reasonably

to Ge. For P in Ge their isotpic substitution model predicts the local mode frequency to be 1.27 ν_1 while the observed frequency of 343 cm^{-1} is only about 1.14 ν_1. Also, here, the isotopic substitution is not an adequate model and changes in force constants are required to describe the situation.

The authors thank Worth Allred for advice and assistance in the growth of the crystals used.

REFERENCES

III-1. For example, see O. G. Lorimor and W. G. Spitzer, J. Appl. Phys. 38, 3008 (1967); S. Ibuki, H. Komiya, A. Mitsuishi, A. Manabe, and H. Yoshinaga, Proc. Int. Conf. of the II-VI Semiconducting Compounds, Brown University, 1967; M. Balkanski and M. Nazarewicz, J. Phys. Chem. Solids, 25, 437 (1964).

III-2. D. W. Feldman, M. Ashken, and J. H. Parker, Phys. Rev. Letters 17, 1209 (1966).

III-3. W. G. Spitzer and M. Waldner, J. Appl. Phys. 36, 2450 (1965).

III-4. Unpublished work of one of the authors, A. Cosand.

III-5. H. Reiss, C. S. Fuller, and F. J. Morin, Bell System Tech. J., 35, 535 (1956).

III-6. M. Waldner, M. A. Hiller, and W. G. Spitzer, Phys. Rev. 140, A172, (1965).

III-7. V. Tsvetov, W. Allred, and W. G. Spitzer, Proc. Int. Conf. on Localized Excitations in Solids, Irvine (Plenum Press, New York, 1968); V. Tsvetov, W. Allred and W. G. Spitzer, Appl. Phys. Letters 10, 326 (1967).

III-8. R. J. Elliott and P. Pfeuty, J. Phys. Chem. Solids, 28, 1627 (1967).

III-9. P. G. Dawber and R. J. Elliott, Proc. Phys. Soc. 81, 453 (1963).

IV. Lithium-Boron Defect Pairs in $Si_{1-x}Ge_x$ Alloys

Ge_xSi_{1-x} alloys have been grown from the melt for $0 \leq x \leq 0.1$ and with a B concentration near 10^{19} cm^{-3}. Samples were diffused with Li at elevated temperatures until sufficiently well compensated that infrared transmission measurements could be made. Localized vibrational modes of B-Li pairs in Si have been previously observed by infrared absorption in several studies. Measurements have been made of these same infrared absorption bands due to B-Li pairs for $0 \leq x \leq 0.1$. All of the local mode bands observed show inhomogeneous line broadening and have lower frequencies for larger values of x.

Isolated boron atoms in silicon sit substitutionally in a tetrahedral site; the symmetry is high enough that the localized vibrational mode is completely degenerate and infrared absorption occurs at only one frequency. When electrical compensation is effected with Li, the Li and boron exist almost entirely as B-Li pairs at room temperature. The symmetry of the B-Li pairs is such as to partially lift the degeneracy of the B local mode and two absorption bands are observed: presumably one corresponds to a single degenerate mode along the B-Li axis, the other to a doubly degenerate transverse mode. One absorption band due to Li in the B-Li pair is seen; in this model a second band should exist (and is seen in the analogous case of Li-Ga pairs in Ge) but apparently its frequency lies in the lattice continuum which would result in a line too broad and weak to be observed.

It had been expected that new bands might appear, corresponding to boron on sites with one Ge and three Si nearest neighbors; an assymmetrical

broadening of the narrower of the two B-Li pair bands may be evidence that this actually occurs. If, as is assumed, the assymetrically broadened line corresponds to the single degenerate axial mode, then it appears that in the case of a Ge-B-Li complex, the three atoms prefer to lie along a single axis, as any other configuration would tend to split the degeneracy of the transverse mode.

V. Localized Vibrational Modes of Substitutional Defect Pairs in Silicon and Lithium Induced Donor Precipitation

A. Introduction

There have been many recent studies[V-1] of the effect of impurities, both substitutional and interstitial, on the vibrational modes of crystals. The conditions for introducing high frequency localized vibrational modes have been discussed in the literature, and experimental observation of infrared absorption bands associated with localized modes have been reported for a number of systems. Several cases have involved impurities, with concentrations ranging between 10^{16} and 10^{20} cm^{-3}, in semiconductor crystals. In many cases the impurity used is an electrical dopant, and the resulting absorption from the large free carrier concentration must be reduced by the introduction of an electrically compensating impurity. This is the reason for some cases involving pairs of impurities.

Of interest to the present study is the experimental work done with B and B-Li impurities in Si. Measurements[V-2] place the triply degenerate localized mode for isolated substitutional B near 624 cm^{-1} at liquid nitrogen temperature for ^{11}B and 647 cm^{-1} for ^{10}B. Both frequencies are larger than the highest unperturbed silicon phonon frequency of ~ 518 cm^{-1}. When interstitial Li compensates B some rather striking effects have been reported[V-3, V-4]. Most of the triply degenerate B band is split, indicating doubly and singly degenerated modes separated by 90 cm^{-1} with the doubly degenerate modes at higher frequency. In addition a band is observed

slightly above the top of the unperturbed spectrum. The frequency of this mode is dependent upon the Li isotope but insensitive to the B isotope. A qualitative explanation has been offered in which these bands are related to the formation of ion pairs, B_{Si}-Li_i, where B_{Si} is B on a Si site and Li_i is interstitial Li. The point group symmetry at the B and Li sites is reduced from tetrahedral (T_d) to axial (C_{3v}) by the pairing.

This work is an experimental study of Si doped heavily with B and largely compensated with a substitutional donor impurity, i.e. P, As, or Sb. The compensation is completed by diffusing Li. New absorption bands have been observed which can be attributed to B-P, B-As, and B-Sb nearest neighbor pairs. In some cases, notably B-P, the strength of some of the absorption bands depends upon the time and temperature of Li diffusion. This latter effect is interpreted in terms of impurity precipitation.

B. Experimental Method

Silicon ingots were pulled from a melt of high purity Si and the desired impurities. The B and Sb were introduced in elemental form while P and As were added as $Ca_3(PO_4)_2$ and $Ca_3(AsO_4)_2$. In most cases B and the donor impurity were added to the melt simultaneously with concentrations adjusted to make the crystal p-type but, where possible, nearly compensated. The B concentration [B] was always $\gtrsim 10^{20}$ cm^{-3} while the donor concentrations varied from near 10^{20} cm^{-3} for [P], $\sim 5 \times 10^{19}$cm^{-3} for [As], and $\sim$2-3 x 10^{19}cm^{-3} for [Sb]. The samples were single crystal or polycrystalline with crystallities of several mms. in dimension. The

B used was enriched ^{11}B, i.e. 98% ^{11}B and 2% ^{10}B. Four point probe measurements of the resistivity ρ gave values consistent with the doping levels. The silicon was diffused with natural Li, i.e. ~93% ^{7}Li and 7% ^{6}Li. The resulting compensated samples had $\rho \gtrsim 100\ \Omega$ cm. The times, temperatures, and conditions for Li diffusion have already been discussed(V-4, V-5) Spectral half widths were always less than 1.0 cm^{-1} wave number and generally near 0.5 cm^{-1}. All optical measurements were made at liquid nitrogen temperature.

C. Experimental Results

1. Localized Mode Frequencies. In Fig. V-1 results were shown for three samples, each doped with ^{11}B a substitutional donor, and Li. The term donor will be used only for the substitutional donor impurity and not for the diffused Li. The bands near 523, 536, 566, 586, 622, and 656 agree closely with bands reported for samples not containing the donor. These absorption bands are related to the presence of B and Li. New bands (V-6) have been observed for each donor, and their positions in Fig. V-1 are indicated by the arrows. There are two bands in each case with a possible third one in the B-As sample. The frequencies depend upon the donor employed. In a B-P crystal the new bands have very nearly the same isotope shift as isolated B band. Measurements at $5^{o}K$ gave nearly the same results as those obtained at nitrogen temperature. The line widths and absorption peak positions as a function of temperature for the new band are, within experimental accuracy, the same as for the isolated B line.

Several B-P doped ingots have been grown and the new bands are present in all cases. An ingot was doped with B and elemental Ca, and Li compensated. The concentration of Ca introduced was the same as that by the $Ca_3(PO_4)_2$ and only B and B-Li bands were observed.

2. Dependence of Absorption Band Intensities on Li Duffusion Conditions. In B-P doped samples the relative intensities of several of the local mode absorption bands are a function of the time and temperature of Li diffusion. The change is indicated in Fig. V-2 for a set of four B-P doped samples. The samples were adjacent to one another in the ingot and all Li diffused at $800^{\circ}C$. The diffusion time ranged from 3 to 15 hours. There is a decrease in strength with increase in the diffusion time for both the 622 cm^{-1} with a concomitant increase in the bands near 656, 566, and 523 cm^{-1}. The relationship between these changes is demonstrated in Fig. V-3 where the change in the 622 cm^{-1} band peak height is plotted against that of the 656 cm^{-1} band. The changes are measured with respect to the second sample from the bottom in Fig.V-2where both bands are nearly the same. Included in Fig.V-3are two samples labeled ($700^{\circ}C$). One was diffused for 8 hours (point with $\Delta 622 = 186\ cm^{-1}$) and the other for 96 hours at that temperature. Within the scatter of the data, the points indicate a linear relation given by $\Delta 622 = -(0.45)\ \Delta 656$. The same result is obtained if the 566 cm^{-1} band is used in place of the 565 cm^{-1}.

No such effect has been observed in the B-As doped samples. The B-Sb samples show a small decrease in band strength for all bands with

longer times of diffusion at 800°C as well as an increase in the apparent background absorption.

D. Discussion of Results

1. Localized Mode Frequencies. Table V-1 lists the local mode absorption bands observed in the present measurements. Frequencies are the position of the peak absorption coefficient. The new bands have been labeled as ^{11}B-P, ^{11}B-As, and ^{11}B-Sb pair bands. The reasons for this assignment are similar to those used to establish the identification of the B-Li pair bands[(V-4)]. The nearly full B isotopic shift, the proximity to the isolated B line, and the shift in frequency with change in donor species indicate the identification of the vibrational modes as ones which primarily involve B motion but the point group symmetry at the B site has been lowered from T_d to C_{3v} by the nearest neighbor substitutional donor. The triply degenerate isolated ^{11}B mode should be split into two bands with one twice the strength of the other. If the donor were 2nd nearest neighbor, the symmetry becomes C_{2v} and three bands could result but with reduced splittings. In the B-P and B-Sb cases only two bands are observed. In the B-As case there is a third band near 627 cm^{-1}. We tentatively ascribe this latter band to an unresolved second nearest neighbor interaction where the remaining structure is under the large 622 isolated ^{11}B line.

The relative strengths of the B-(Donor) bands are difficult to determine as they are weak and close to the strong isolated B and B-Li bands. An estimate is made by assuming the background in the region of

TABLE V-1

Liquid Nitrogen Temperature Frequencies of Absorption Bands

Band	$^{11}B-^{7}Li$	$^{10}B-^{7}Li$	$^{11}B-P$	$^{11}B-As$	$^{11}B-Sb$
B-Li Pair	656.1 ± 0.6	683	---	---	---
Bands	566.1 ± 0.6	586	---	---	---
B Band	622.2 ± 0.5	647	---	---	---
Li Band	523.3 ± 0.5	523.3 ± 0.5	---	---	---
B-Donor	---	---	~ 628	636.7 ± 0.4	642.7 ± 0.3
Bands	---	---	600.1 ± 0.5	603.7 ± 0.3	611.9 ± 0.3
	---	---	---	~ 627	---

B-D bands to be a constant plus the tails of the nearby major bands. The absorption tails are estimated by assuming at each local mode can be represented by a collection of non-interacting harmonic oscillators of resonance frequency ν_o. This model gives an absorption coefficient

$$\alpha = \frac{C}{n} \left\{ \frac{\nu^2}{(1-\nu^2)^2 + \nu^2 \delta^2} \right\},$$

where ν and δ are the frequency and damping constant normalized by the resonance frequency, n the refractive index, and C a constant. It is assumed that n is independent of frequency. Figure V-4 shows the curve fitting for a B-P sample. The only major band close enough to the B-P pair bands to have any effect is the isolated ^{11}B band at 622 cm^{-1}. C/n was adjusted to give α_{peak} = 250 cm^{-1} with δ of 0.008 (5.0 cm^{-1}). Measurements over a more extended frequency range indicate that for this

sample, $\alpha_{background} = 14\ cm^{-1}$. Subtraction of $\alpha_{background}$ and the calculated curve from the measured data points give the dashed curves in Fig. V-4.

The results for estimates of $\int \alpha d\nu$ for the pair bands in several samples are given in Table V-2. While the results are not conclusive, they suggest that the high frequency band is the doubly degenerate one for B-P and B-Sb and the low frequency one for B-As. Comparison of the total integrated absorption of the B-Donor pair bands to that for isolated B gives $\Sigma_{pair} \int \alpha d\nu = 0.1$ to $0.2 \int_B \alpha d\nu$ for both B-P and B-As and 0.4 to $0.5 \int_B \alpha d\nu$ for B-Sb. The difference could arise either from a somewhat larger pairing energy for the B-Sb case or from the equilibrium configuration for B-Sb being characteristic of a somewhat lower temperature. The latter case would imply a larger diffusion constant for Sb than for As and P which is not in agreement with published data.(V-7)

TABLE V-2

Sample	$\int a d\nu$ (cm^{-2})	
	High frequency pair band	Low frequency pair band
B-P	297	133
B-P	200	132
B-As	65	110
B-Sb	120	90

The qualitative conclusions given here are in general agreement with the recent theory of Elliott and Pfeuty[(V-8)]. They calculate the effect of pairs of defects on the lattice modes by using Green's function methods. Of particular interest are their calculations for the frequencies of the localized modes of defect pairs in silicon where one of the defects is B_{Si} and the other a substitutional mass M_2. Their results for no change in force constants are reproduced here in Fig.V-5. The solid lines are for ^{11}B, the dashed for ^{10}B, ω_M the maximum unperturbed Si phonon frequency, and M the Si mass. For the cases studied here the mass defect $\varepsilon_2 < 0$ and only two modes should be observed, those labeled modes 1 and 2 on Fig.V-5. The theory indicates that in both modes B motion dominates. The fact that the observed splitting of modes 1 and 2 is much larger than that given in Fig. V-5 is evidence that a change in force constant is necessary. The increase in frequency of the pair bands as one goes from P to As to Sb is in the same order as the tetrahedral covalent radii which are 1.10, 1.18, and 1.36 Å respectively.[(V-9)]

2. Impurity Precipitation Effects. It was observed that $\Delta 622 = -(0.45)\ \Delta 656 = -(0.45)\ \Delta 566$. With the half widths of 7.0 cm^{-1} for the 656 cm^{-1} band, 4.5 cm^{-1} for 566 cm^{-1} band and 5.0 cm^{-1} for the 622 cm^{-1} band it is observed that the change in $\int \alpha d\nu$ for the isolated B band is equal and opposite in sign to the change in total $\int \alpha d\nu$ for the B-Li pair bands. This result indicates that the total substitutional [B] does not change, and the total absorption strength per center is the same for isolated B and B-Li

pairs. This result, the assumption that the isolated B concentration equals the isolated substitutional P concentration, and the data for B-Li doped samples may be used to express the strength of the bands in terms of the concentration of the different defects. In these estimates the B-D pairs were neglected since their absorption bands indicate the concentrations to be relatively small.

The results of Fig.V-2are consistent with a model involving P precipitation or any other process which removes P as an electrically active dopant. From the strength of the 622 cm^{-1} band, the substitutional [P] is found to decrease from 9×10^{19} cm^{-3} to $\sim 1.4 \times 10^{19}$ cm^{-3} after 15 hours of Li diffusion at $800^{\circ}C$. It is known[V-10] that the solid solubility of a donor may be considerably enhanced by a large concentration of acceptors. Annealing of B-P doped samples for 17 hours at $740^{\circ}C$ had no effect on either the resistivity or on the local mode strengths obtained after Li diffusion. During Li diffusion, Li compensates the excess [B] which leads to a decrease in the solubility of P to a value near that in Si without acceptors. Processes of precipitation of P in Si and in Ge-Si alloys have been reported[V-11, V-12] for concentrations similar to those used in the present experiments. At $800^{\circ}C$ the time constant for achieving the equilibrium [P] is $\sim$10 hours while at $700^{\circ}C$ the time constant $\gtrsim 1000$ hrs. These time constants are only approximate as the data are not sufficient to establish the kinetics of the process. Unfortunately, the present authors have been unable to find data on the P solid solubility in Si at $800^{\circ}C$.

The B-As doped samples with [As] of $5 \times 10^{19} cm^{-3}$ did not show any decrease in [As] with Li diffusion at $800^{o}C$ indicating that the As solid solubility is above this concentration.

In the B-Sb case the [B] $\sim 1.9 \times 10^{20} cm^{-3}$ and [Sb] $\sim 2.5 \times 10^{19} cm^{-3}$. Although changes are small compared to those observed in the B-P case, comparison of samples Li diffused at $800^{o}C$ indicates a decrease of ~ 20% in the isolated Sb concentration as a result of long term diffusion. The Sb concentration is close to the published(V-13) solid solubility data at $800^{o}C$ which indicates $\sim 2 \times 10^{19} cm^{-3}$. In addition, a decrease is observed in the total substitutional B concentration to $\sim 1.4 \times 10^{20} cm^{-3}$. This concentration is close to the [B] in the B-P doped samples where no B precipitation was observed.

Mr. V. Tsvetov, a participant of the Educational and Scientific Exchange Program of the USA-USSR, returned to the Soviet Union before the completion of the work described in this section. He is continuing to investigate some aspects of this work as part of his doctoral program at the Electrotechnical Institute of Leningrad, USSR.

REFERENCES

V-1. For a discussion of this topic see A. A. Maradudin, Solid State Physics (Edited by F. Seitz and D. Turnbull, Academic Press, New York, 1966), vol. 18, 273.

V-2. J. F. Angress, A. R. Goodwin, and S. D. Smith, Proc. Roy. Soc. (London) 287A, 64 (1965).

V-3. M. Balkanski and W. A. Nazarewicz, J. Phys. Chem. Solids 27, 671 (1966).

V-4. M. Waldner, M. A. Hiller, and W. G. Spitzer, Phys. Rev. 140, A172 (1965); also W. G. Spitzer and M. Waldner, J. Appl. Phys. 36, 2450 (1965).

V-5. E. M. Pell, J. Phys. Chem. Solids 3, 77 (1957).

V-6. V. Tsvetov, W. Allred, and W. G. Spitzer, Appl. Phys. Letters, 10, p. 326 (1967).

V-7. H. Reiss and C. S. Fuller, Semiconductors (Edited by B. Hannay, Reinhold Publishing Co., New York, 1959), p. 244.

V-8. R. Elliott and P. Pfeuty, J. Phys. Chem. Solids, 28, 1627 (1967).

V-9. L. Pauling, The Nature of the Chemical Bond (Cornell Univ. Press, Ithaca, New York, 1960), p. 246.

V-10. H. Reiss, C. S. Fuller, and F. J. Morins, Bell System Technical Journal 35, 535 (1956).

V-11. M. L. Joshi and S. Dash, IBM Journal of Research and Development 10, 446 (1966).

V-12. L. Ekstrom and J. P. Dismukes, J. Phys. Chem. Solids 27, 857 (1966).

V-13. F. A. Trumbore, Bell System Technical Journal 39, 205 (1960).

VI. Theoretical Calculations of One- and Two-Phonon Optical Absorption from Boron Impurities in Silicon

It is well known that in homopolar crystals such as silicon, there is no first order infrared absorption. There is a second order spectrum, which has been studied by Lax and Burstein (1955), who explained it in terms of the second order dipole moment, since the anharmonicity was unable to provide a mechanism for it. In the present paper we are concerned with the first and second order infrared absorption of boron-doped silicon.

We have calculated the absorption corresponding to the excitation of electromagnetic radiation of the following types of vibrations (which occur near the impurity site):

1) excitation of a local mode vibration;
2) excitation of a perturbed band mode;
3) simultaneous excitation of two local mode quanta (overtones);
4) simultaneous excitation of a local mode and a perturbed band mode (combination tone).
5) simultaneous excitation of a local mode and an unperturbed band mode (combination tone);

These types of absorption are absent in the perfect lattice and (except for 2) their frequencies depend strongly on the boron mass. We do not calculate the second-order absorption arising from simultaneous excitation of two band modes. This will be weak and of the same general structure as

the intrinsic second-order absorption.

We must point out that in calculating with a model system containing only boron as the doping agent we are dealing with a system on which experimental data is not readily available because of free carrier absorption. In practice the boron, which acts as an acceptor, must be compensated by donors, with which it may aggregate into pairs of lower symmetry, and more complex properties, than the isolated boron centers we are dealing with here. Nevertheless, these calculations should serve as a useful starting point for understanding the intensity of absorption in compensated boron-doped silicon.

Since the details of the calculations have been published in articles #3 and 4 which are listed in the Introduction to this report, they will not be reproduced here. The conclusions, however, may be briefly stated as follows: The simplified model employed gives values for the absorption cross section of the fundamental and the first overtone which are in order of magnitude agreement with experiment. Moreover, calculations for the band modes and the combination modes seen to agree qualitatively with the experimental data.

FIGURE CAPTIONS

I-1. Phonon spectrum of a pure zincblende lattice (GaAs).

I-2. Absorption spectra for boron-and lithium-doped silicon: (A) high-purity silicon; (B) boron and ^{6}Li doping; (C) ^{10}B and ^{7}Li; (D) ^{11}B and ^{7}Li.

II-1. Transmission spectra (% Transmission vs wave number) for unirradiated sample 1A.

II-2. Transmission spectra for irradiated sample 1R.

II-3. Transmission spectra for irradiated sample 2R.

II-4a. Absorption spectra measured at room temperature for irradiated sample 4R.

II-4b. Absorption spectra measured at room temperature for irradiated sample 4R, after higher temperature annealings.

II-5a. Absorption spectra measured at room temperature for unirradiated sample 5B.

II-5b. Absorption spectra measured at room temperature for unirradiated sample 5B, after higher temperature annealings.

II-6. Transmission spectra measured at room temperature for unirradiated sample PFL-1. (Note: The discrepancies around $\nu \sim 4300\ cm^{-1}$ and $\nu \sim 1750\ cm^{-1}$ are due to change of gratings).

II-7. Absorption spectra near 2.0 μ measured at liquid-nitrogen temperature with background substracted:
(A) From sample 4R after annealed at 550°C for 30 min.;
(B) From sample 5B after annealed at 550°C for 30 min.;
(C) From the result by Fan and Ramdas (ref. II-3).

II-8. Transmission spectra measured at room temperature for samples 4R and 5B after annealed at 600°C for 30 min. and 24 hours.

II-9. Solubility of lithium in silicon and temperature dependence of certain features of precipitation curve. (From ref. II-6).

III-1. Absorption coefficient of liquid-nitrogen temperature vs wave number for germanium samples: (1) P and Ga doped, ^{7}Li diffused; (2) Ga, As and Sb doped. ^{7}Li diffused; (3) Ga, As and Sb doped, ^{6}Li diffused; (4) pure Ge. Varying amounts of background absorption are the result of imperfect compensation.

V-1. Absorption spectra for silicon doped with ^{11}B and a substitutional donor. Sample have been lithium diffused. The donors are phosphorous (P), arsenic (As), and antimony (Sb).

V-2. Absorption spectra for B-P doped silicon. The samples are lithium diffused for times (t_D) as indicated.

V-3. Comparison of the change of absorption band strength between 656 cm^{-1} band and 622 cm^{-1} band.

V-4. Curve fitting for a B-P doped silicon sample by using a Lorentzian oscillator model.

V-5. Frequencies of localized modes of defect pairs in silicon assume no change in force constants, where one of the defects is B_{Si} and the other a substitutional mass M_2. The solid lines are for ^{11}B, the dashed for ^{10}B, ω_M the maximum unperturbed silicon phonon frequency.

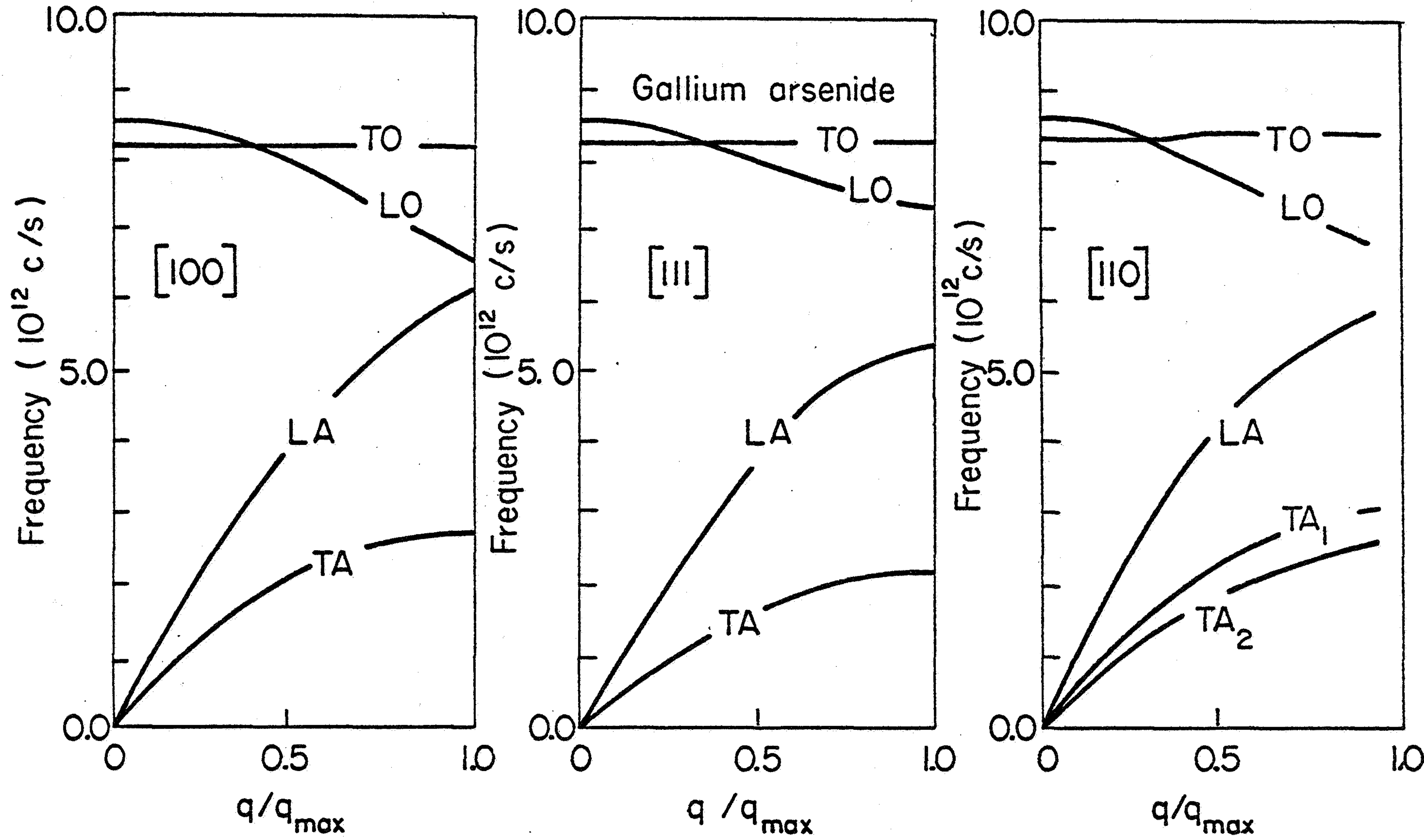

Fig. I - 1

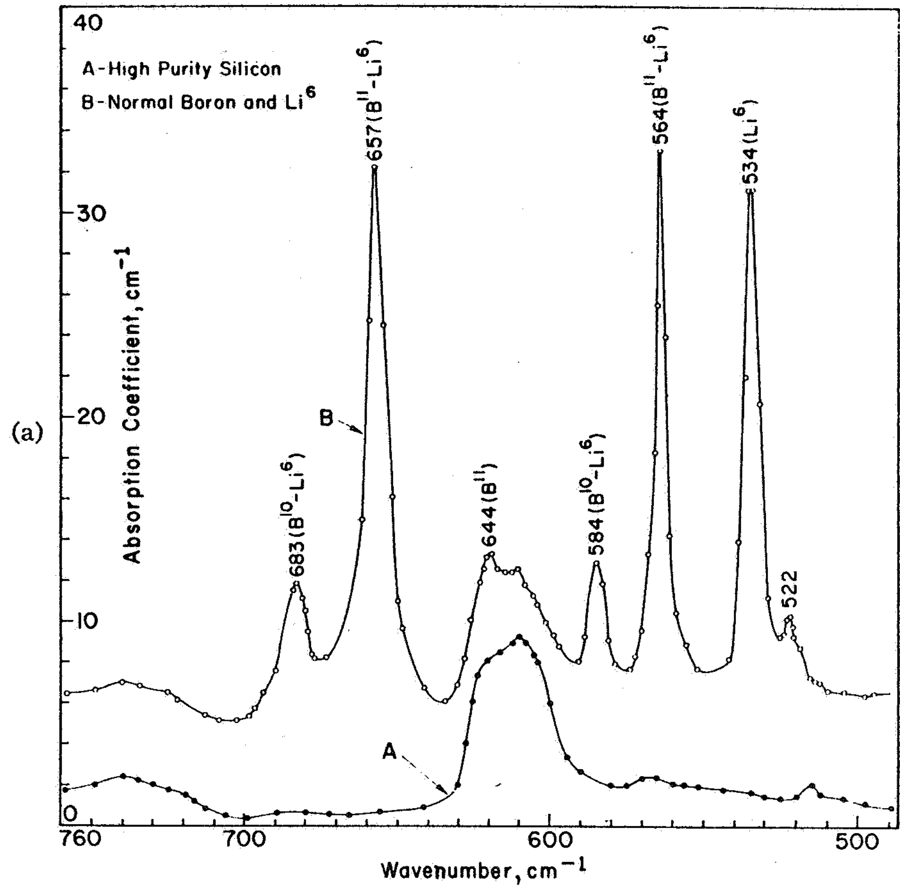

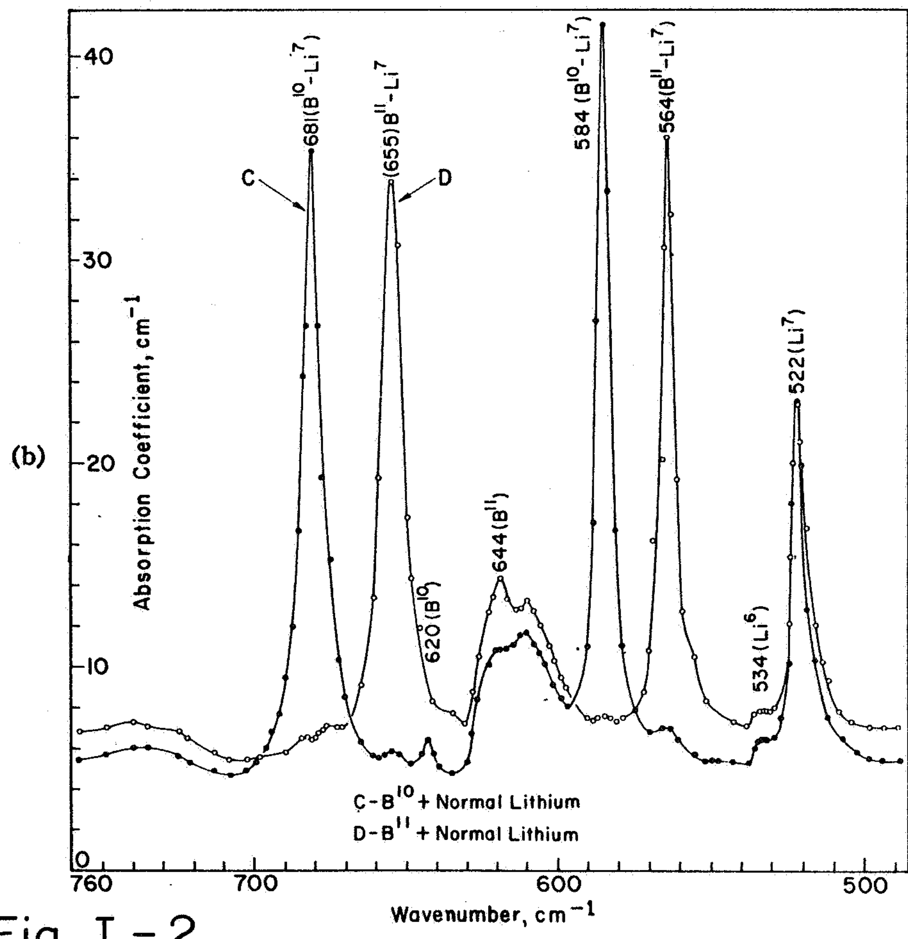

Fig. I - 2

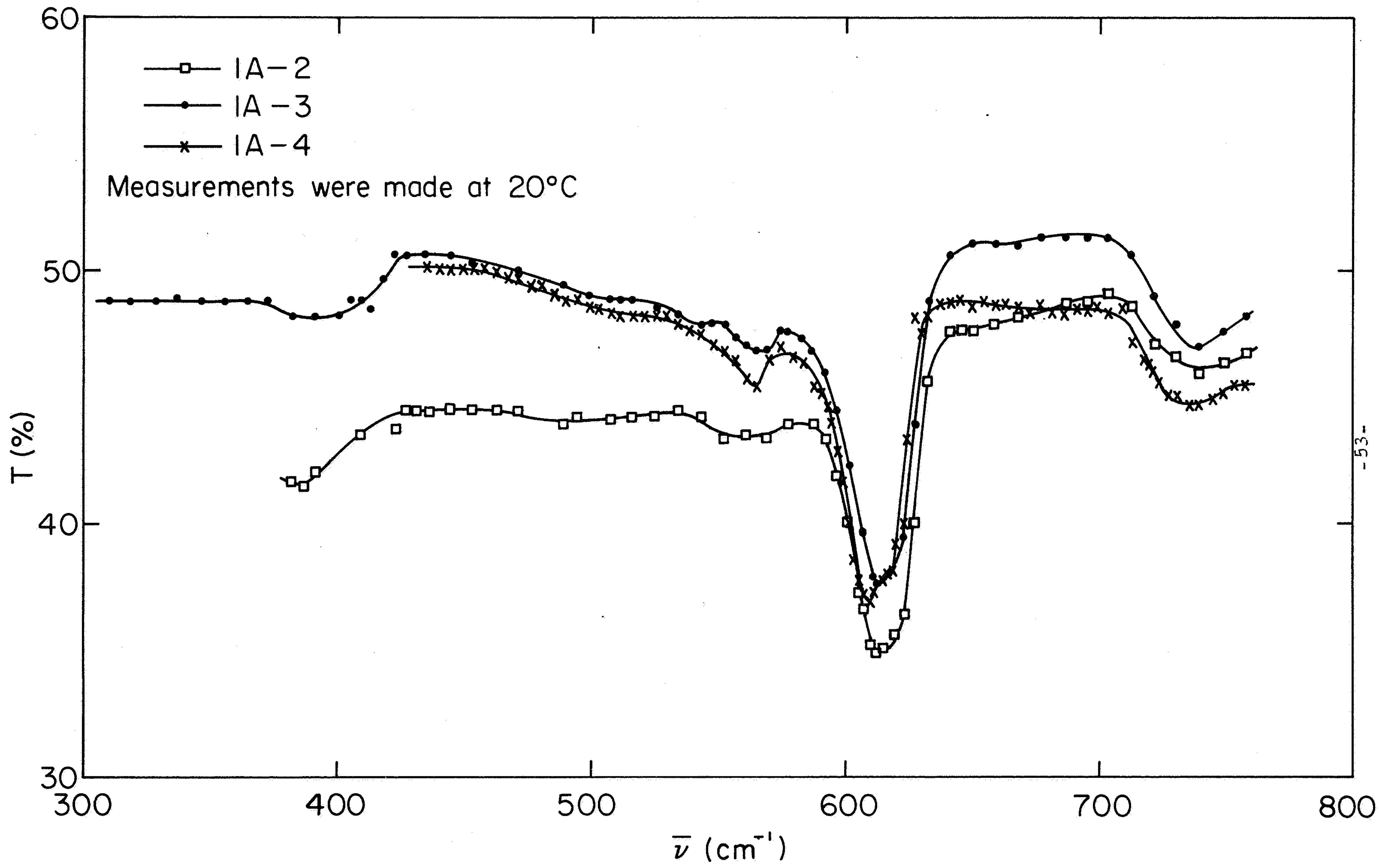

Fig. II-1

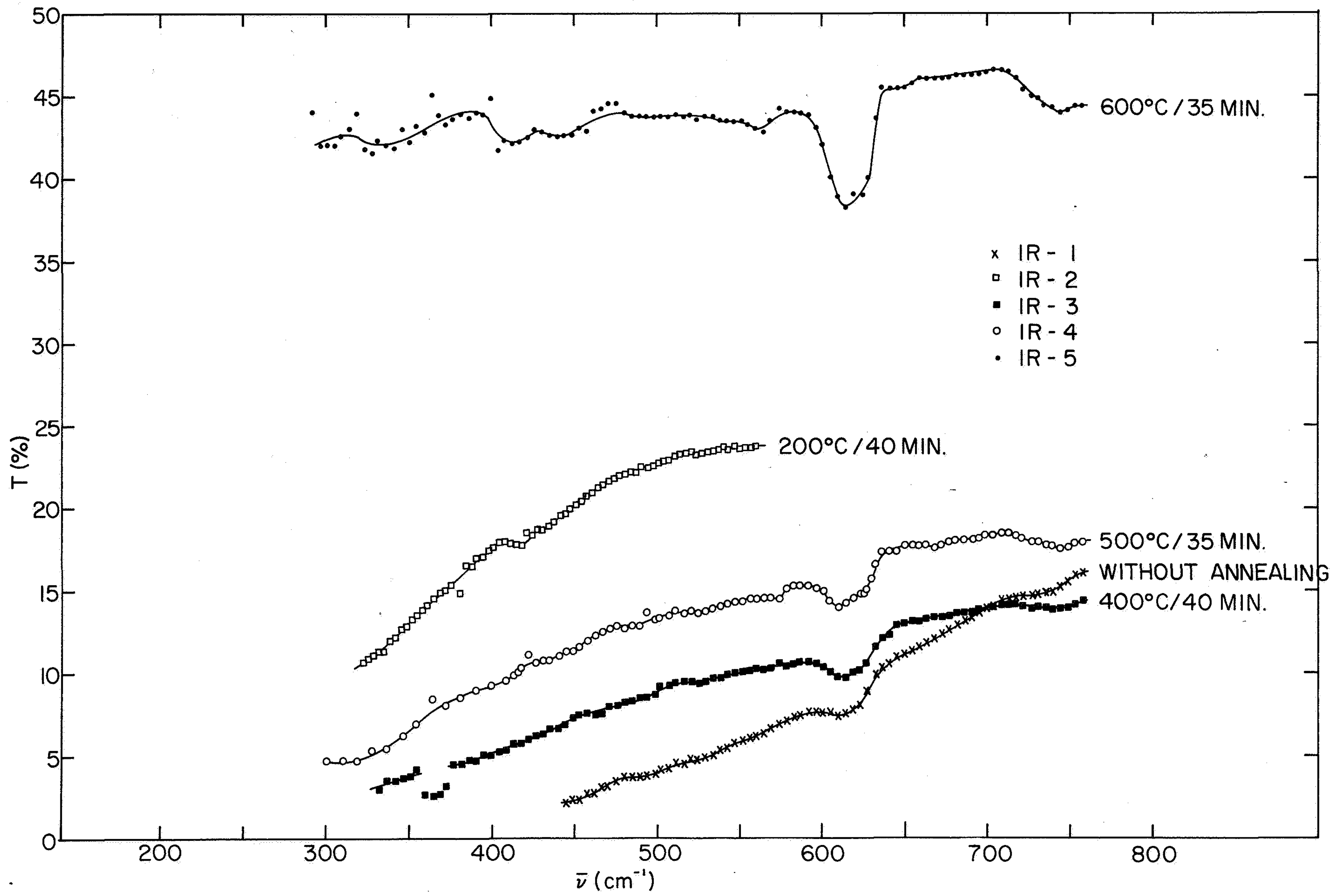

Fig. II-2

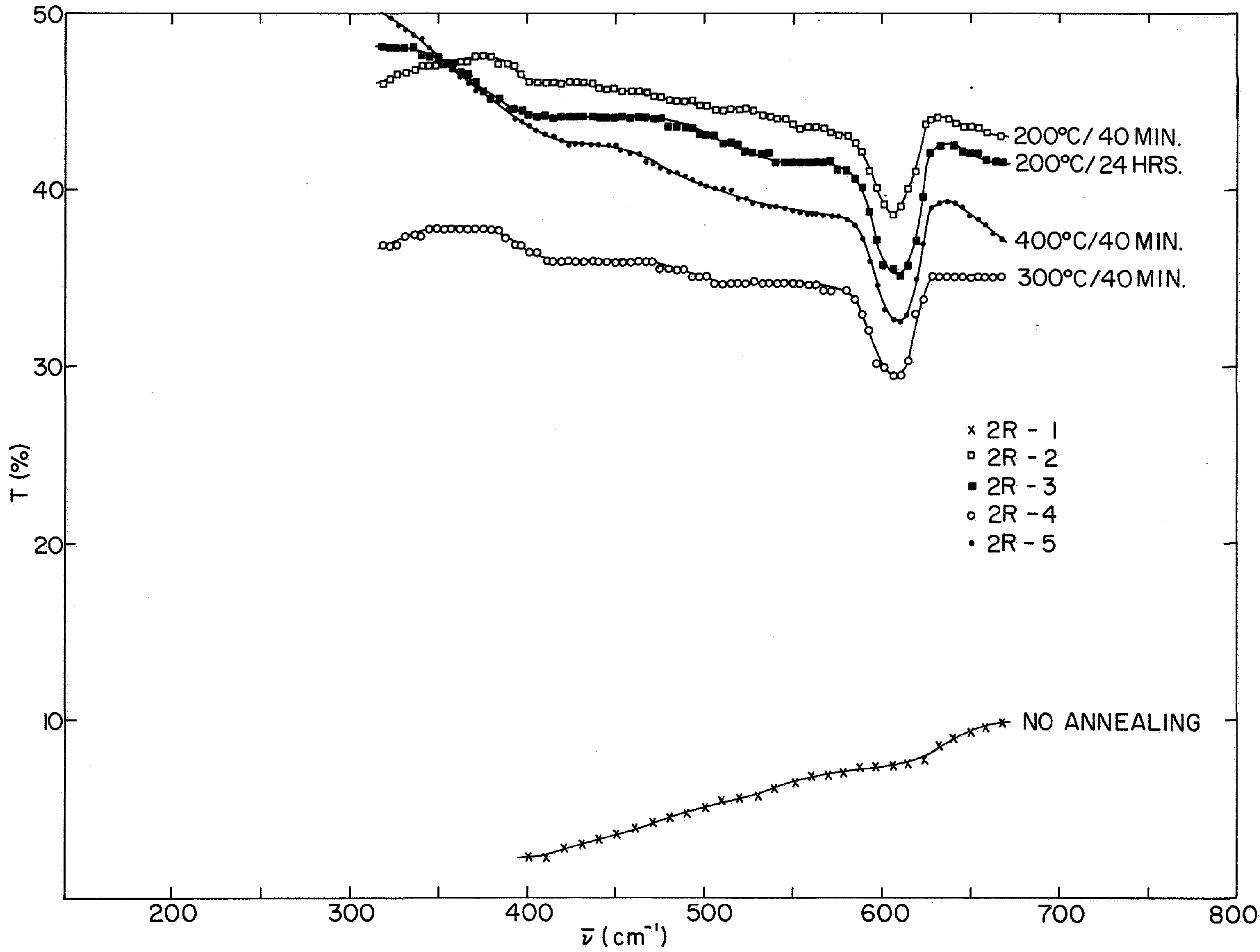

Fig. II-3

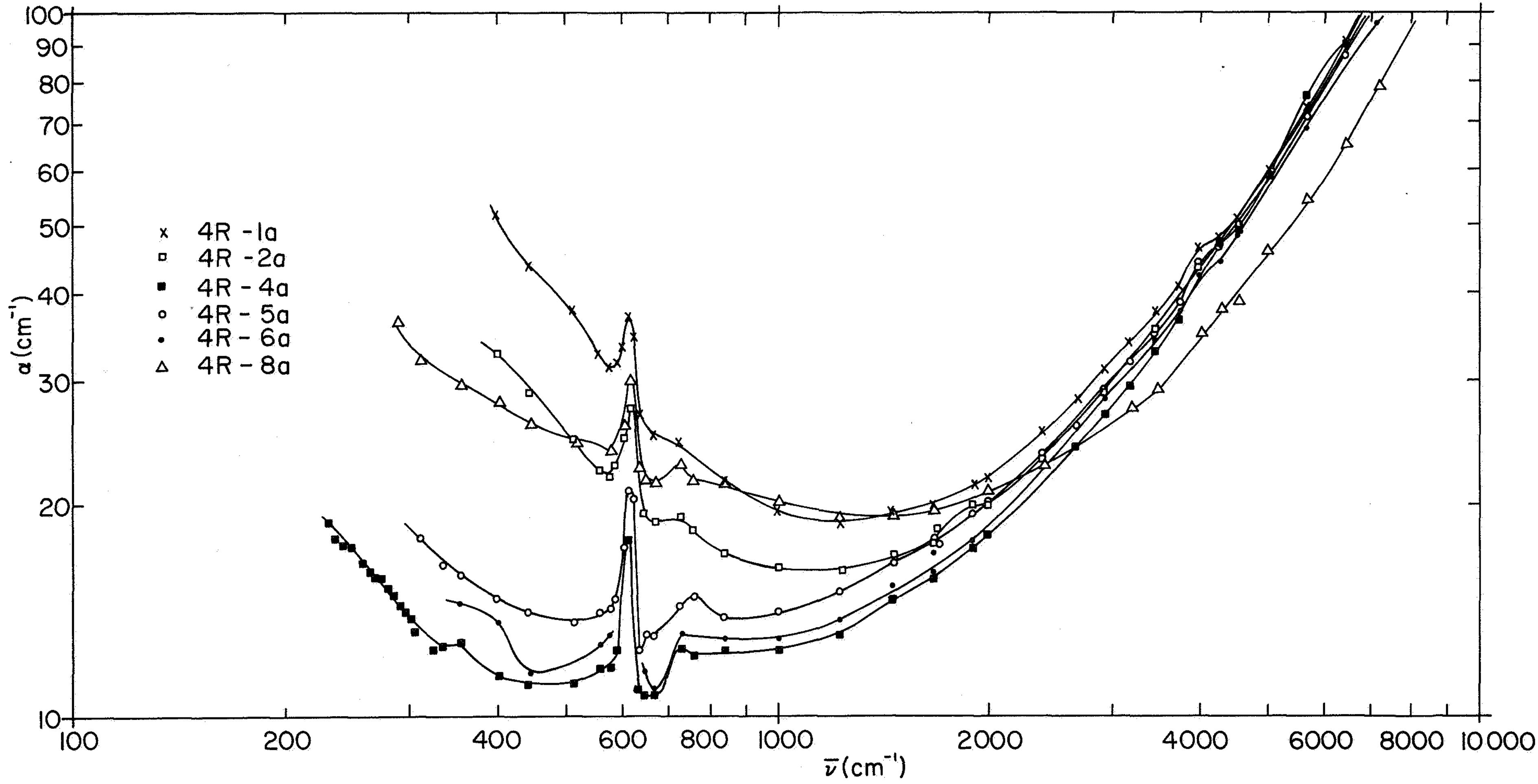

Fig. II - 4a

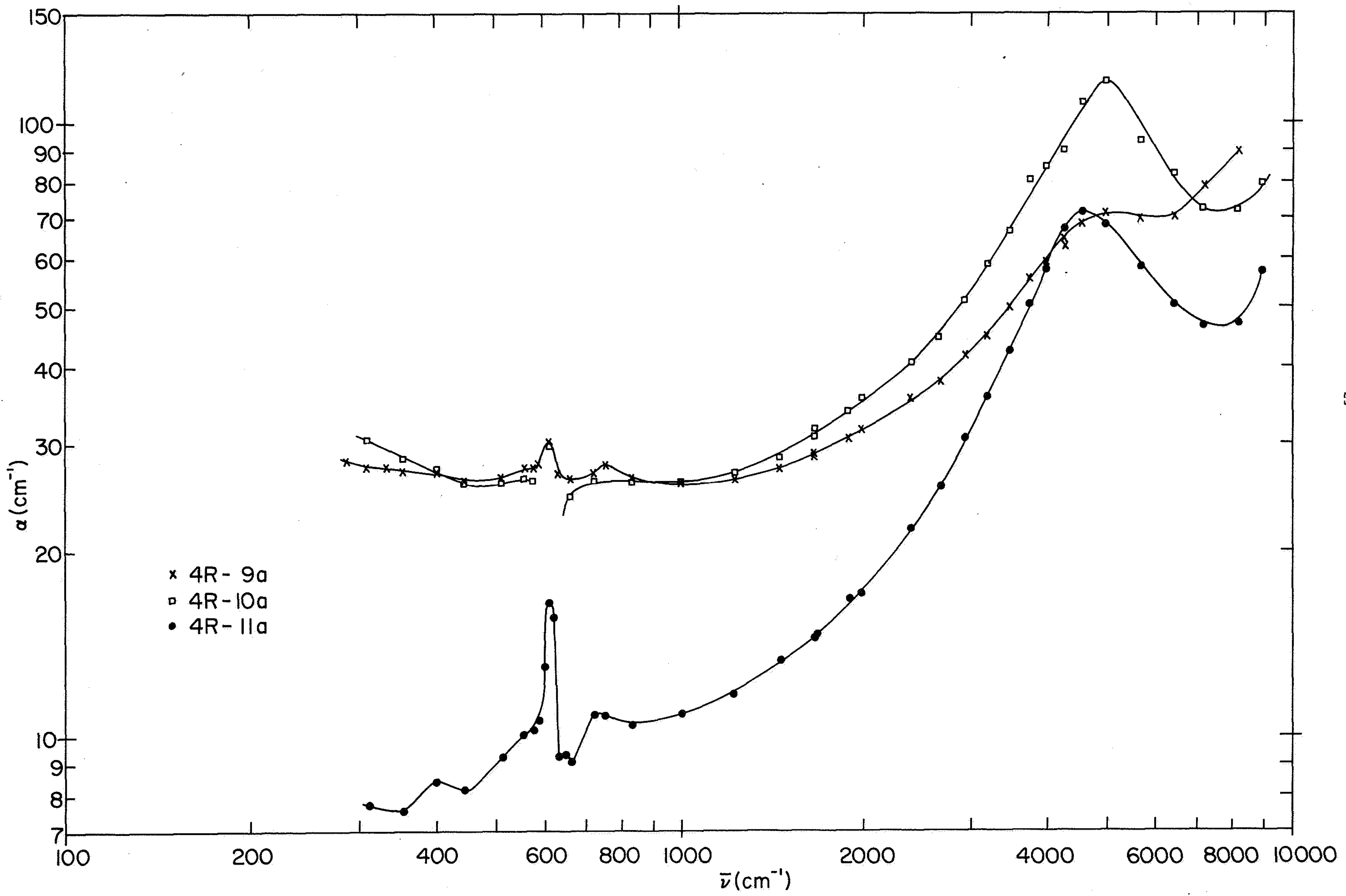

Fig. II - 4b

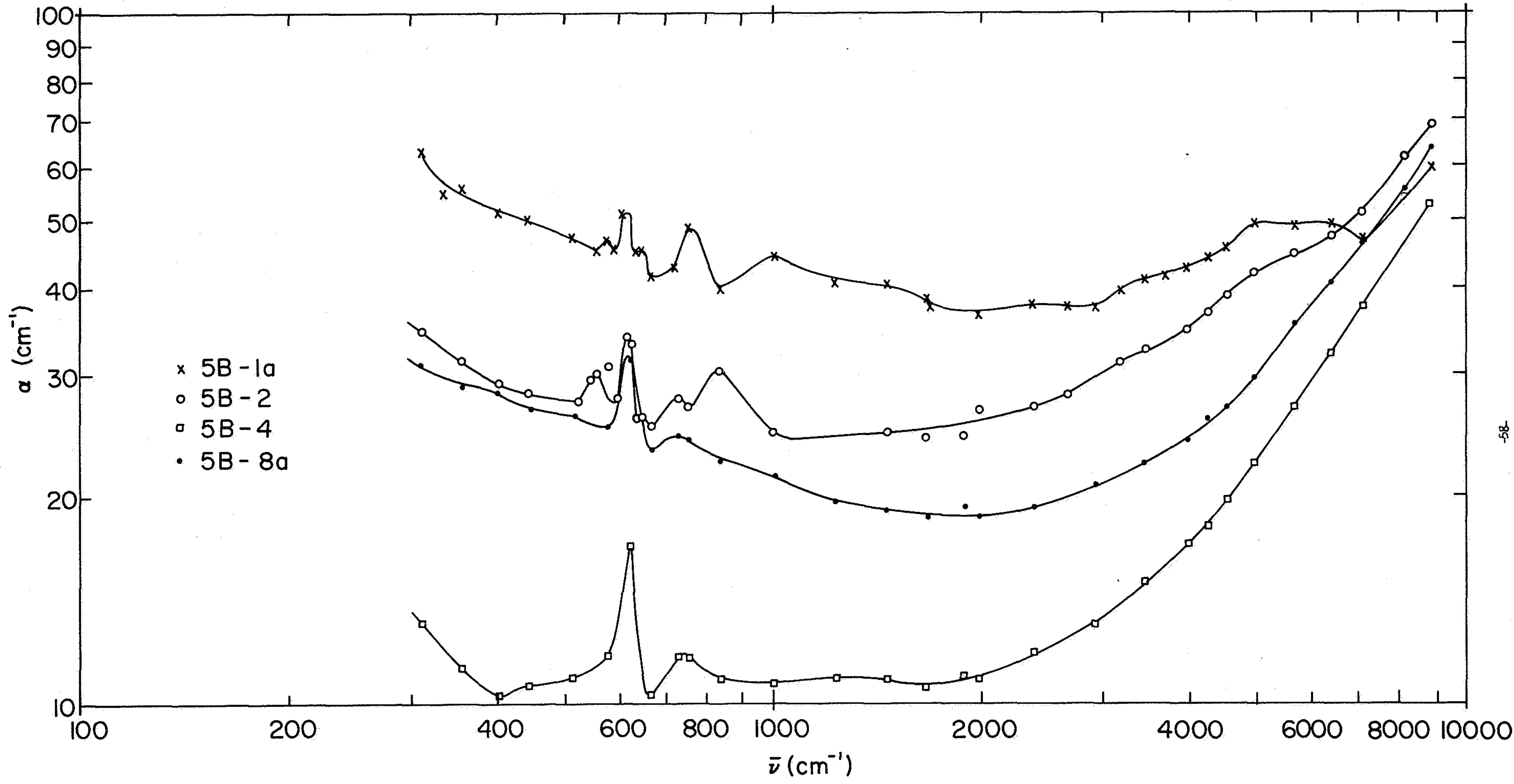

Fig. II -5a

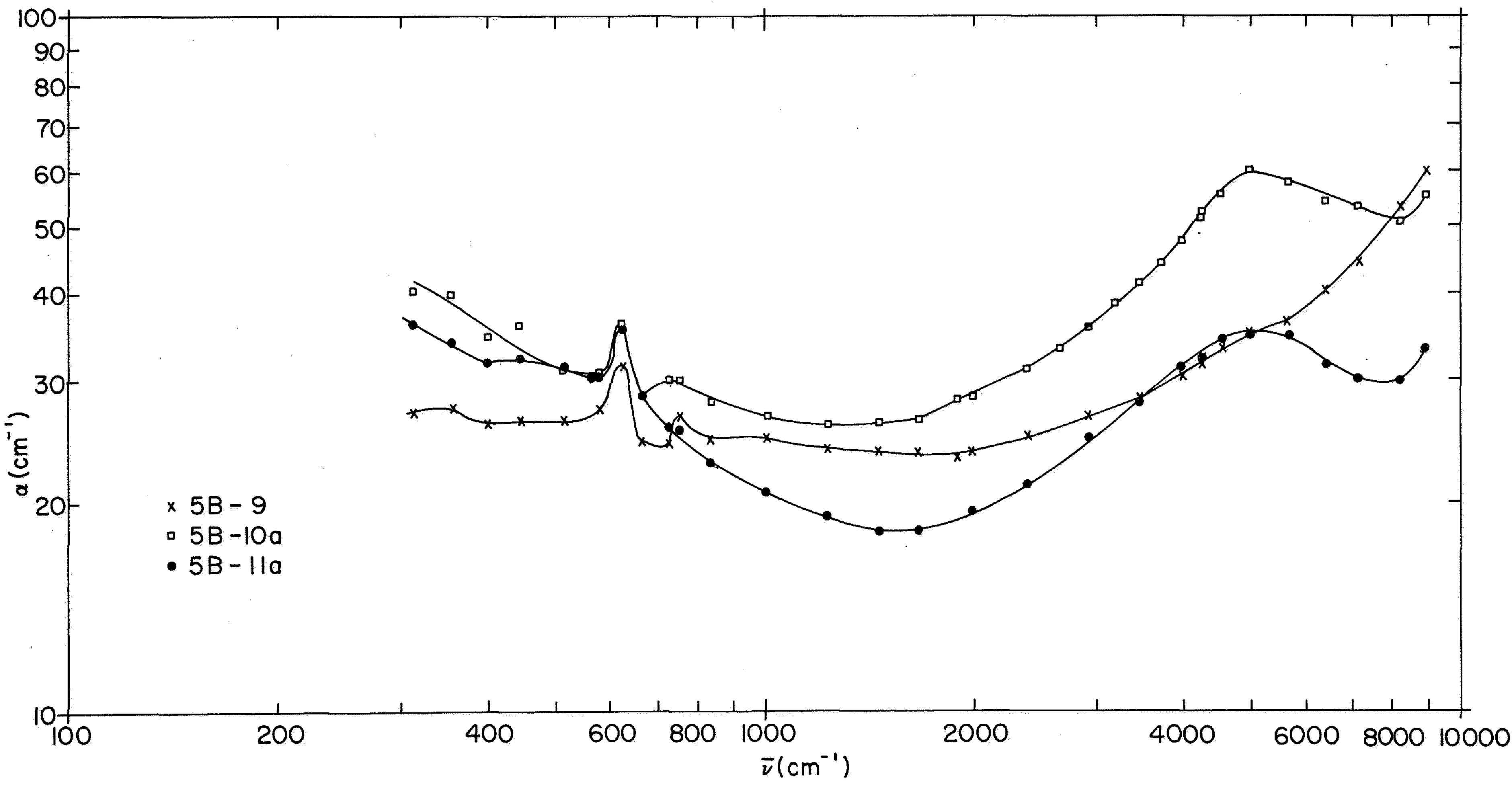

Fig. II - 5b

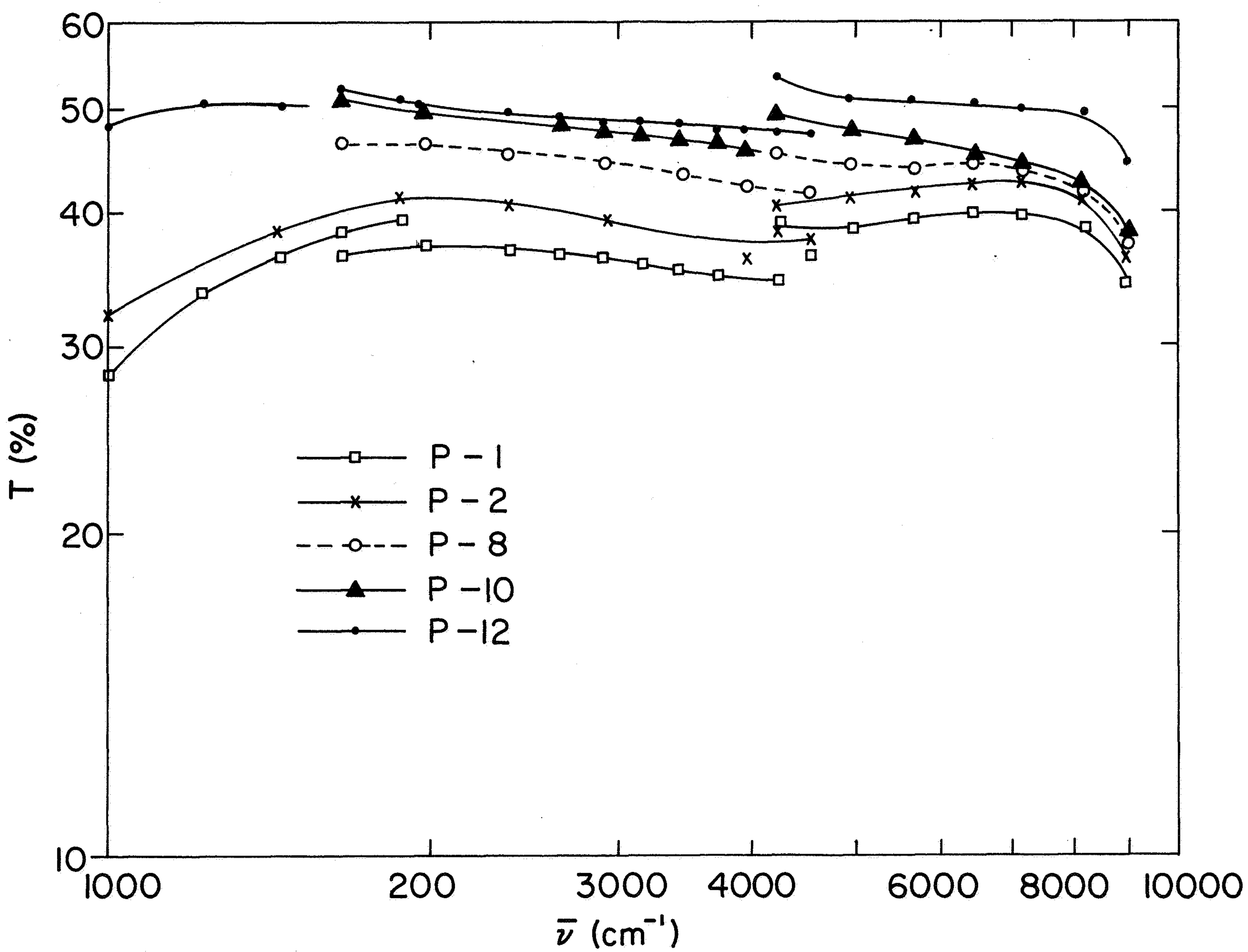

Fig. II − 6

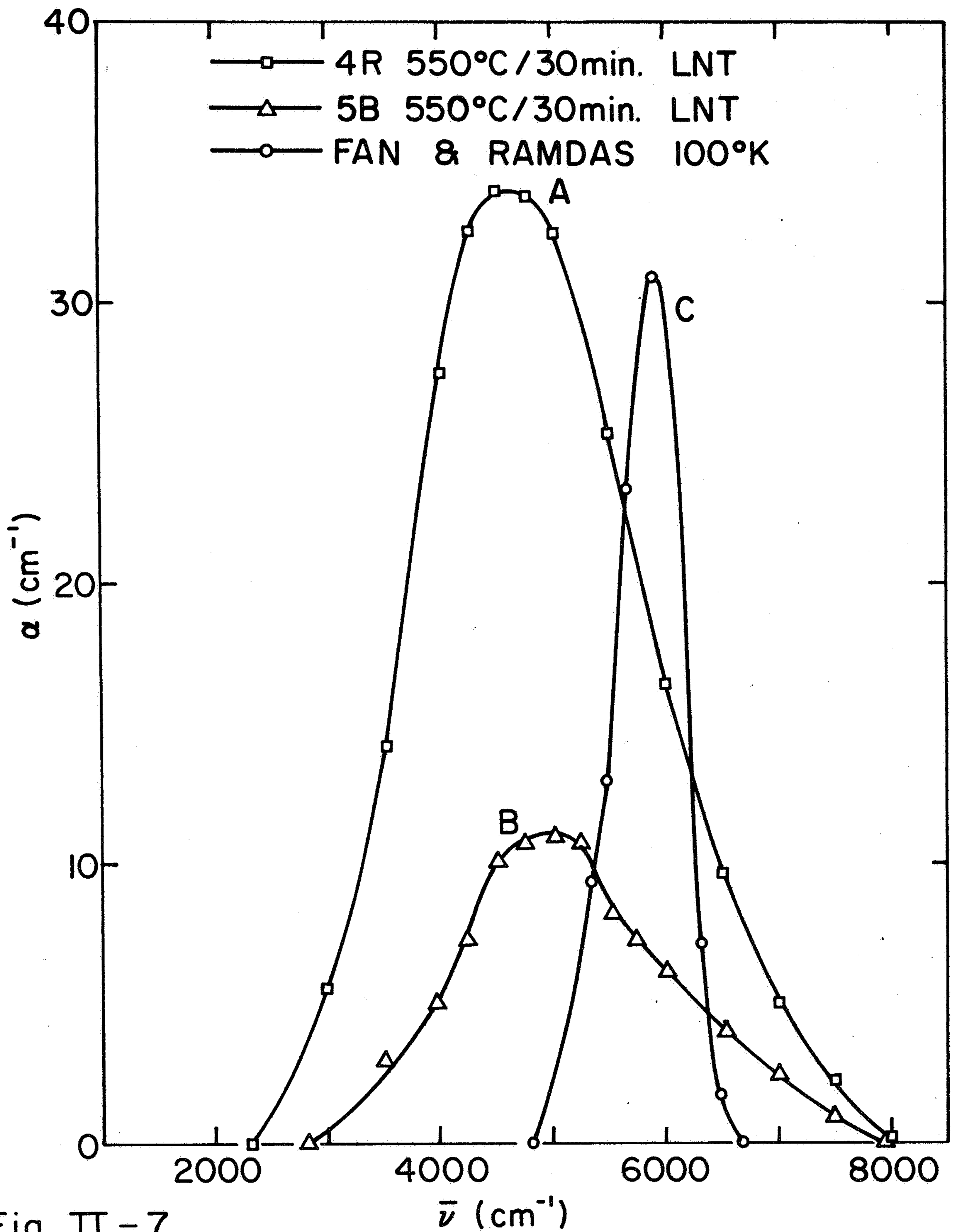

Fig. II-7

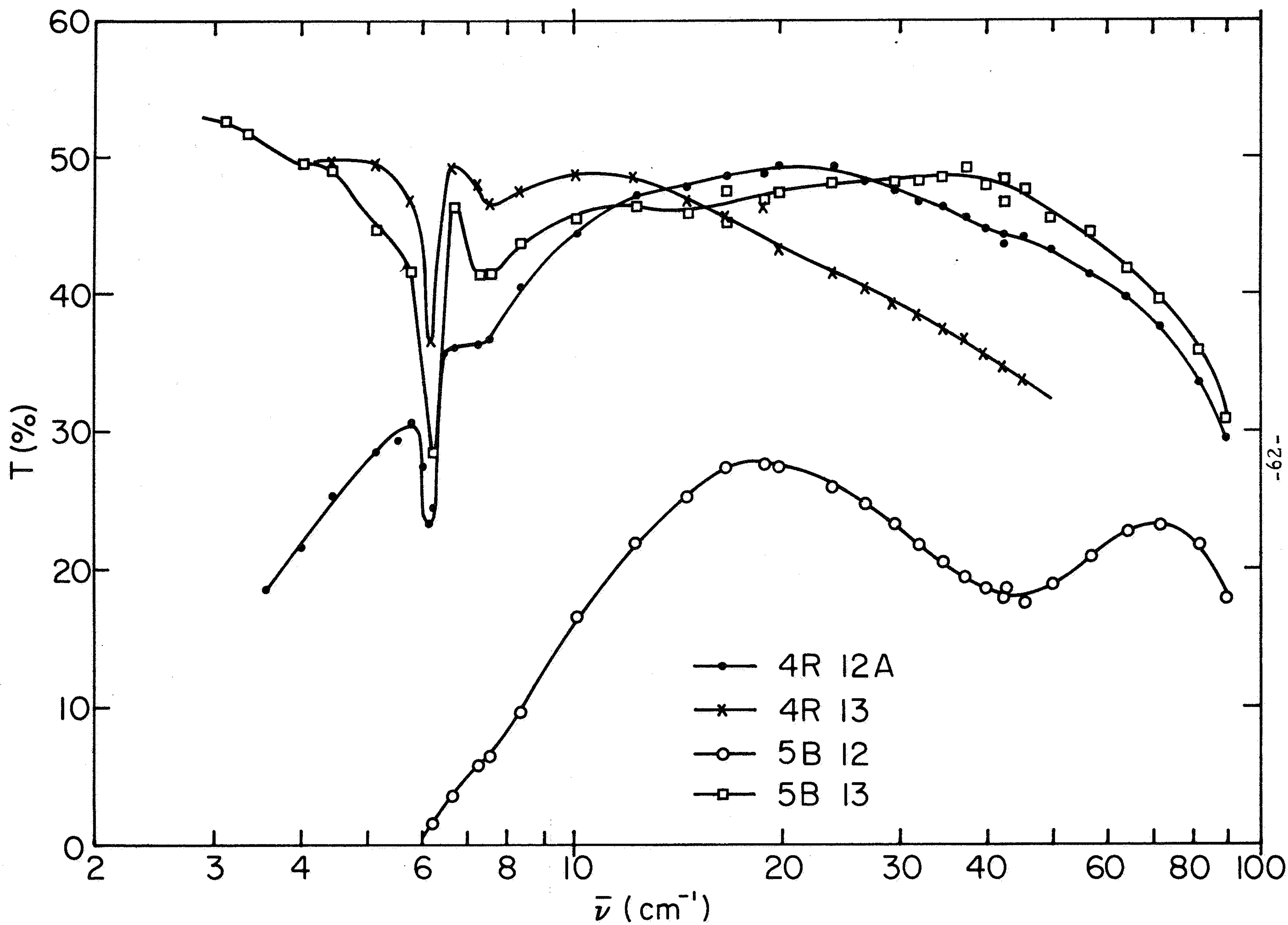

Fig. II − 8

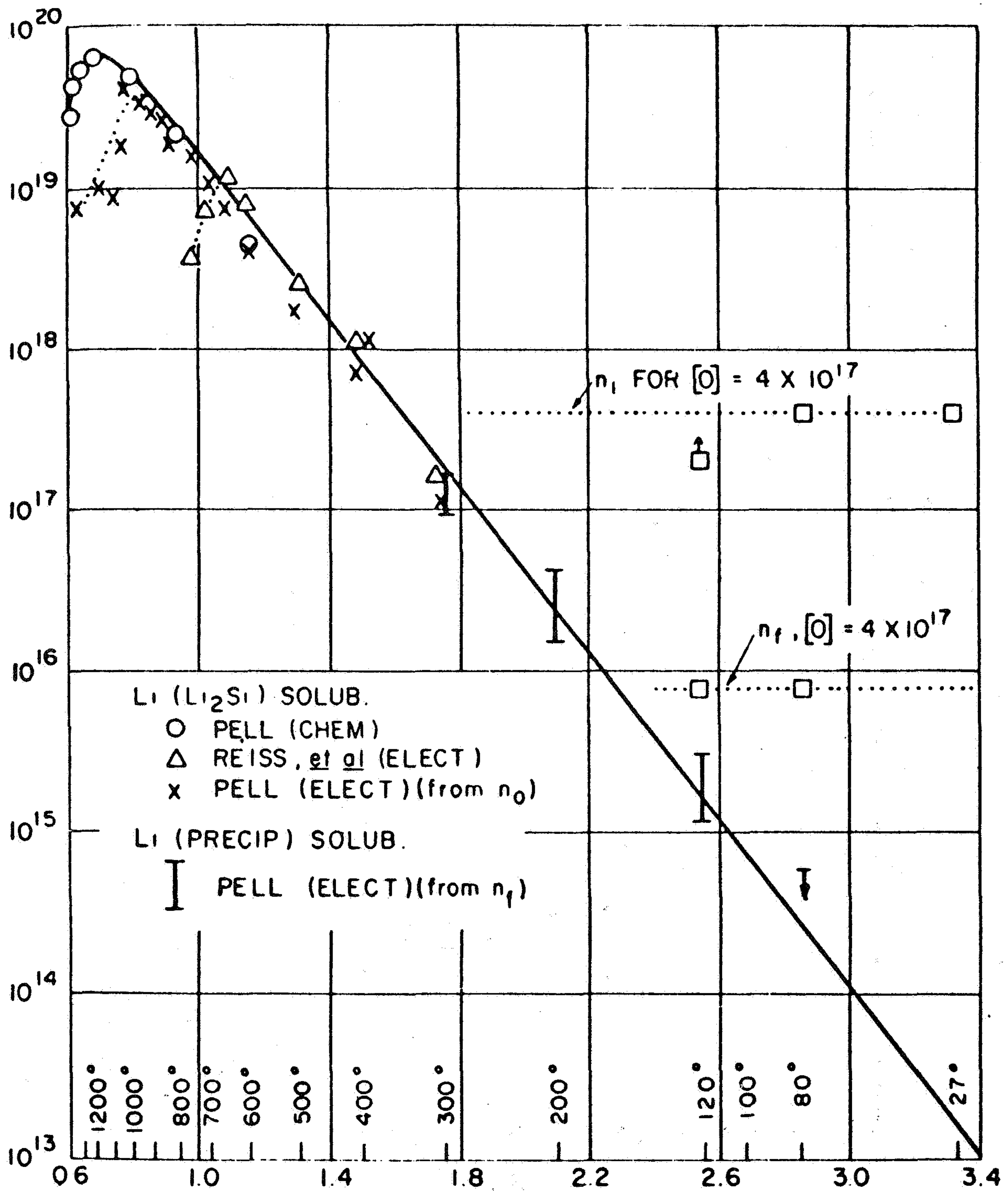

Fig. II – 9

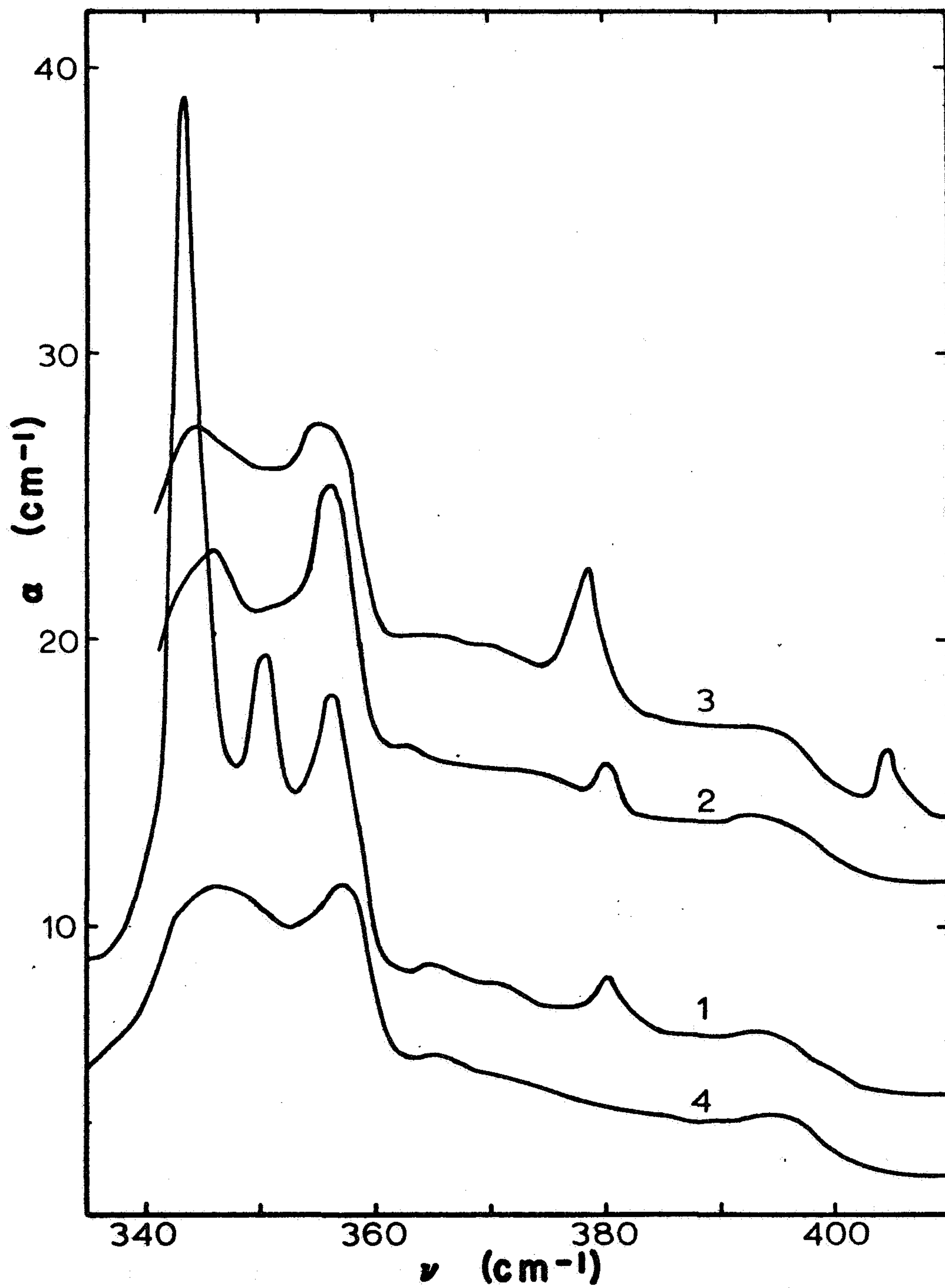

Fig. III-1

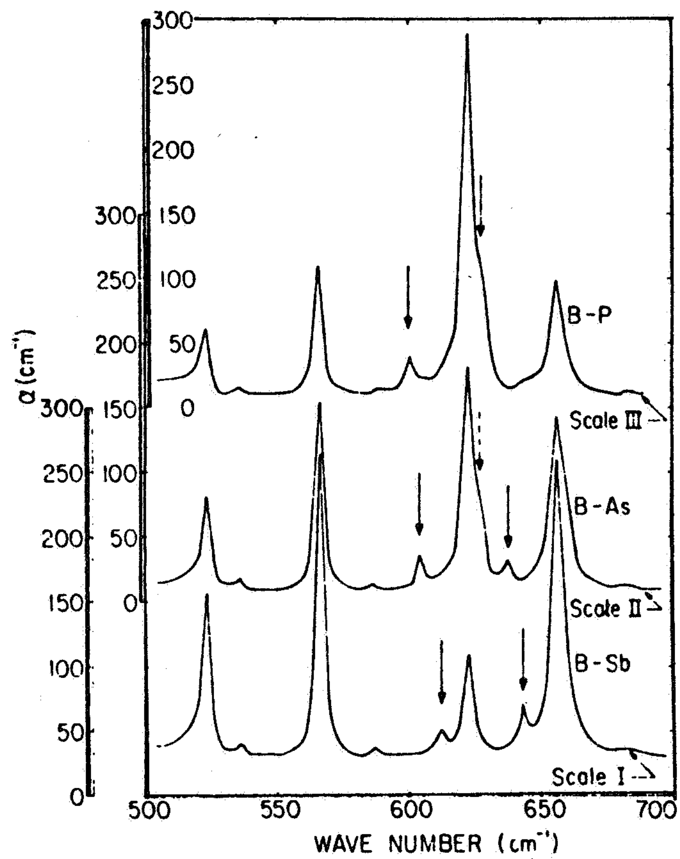

Scale I
Scale II
Scale III

Fig. V - 1

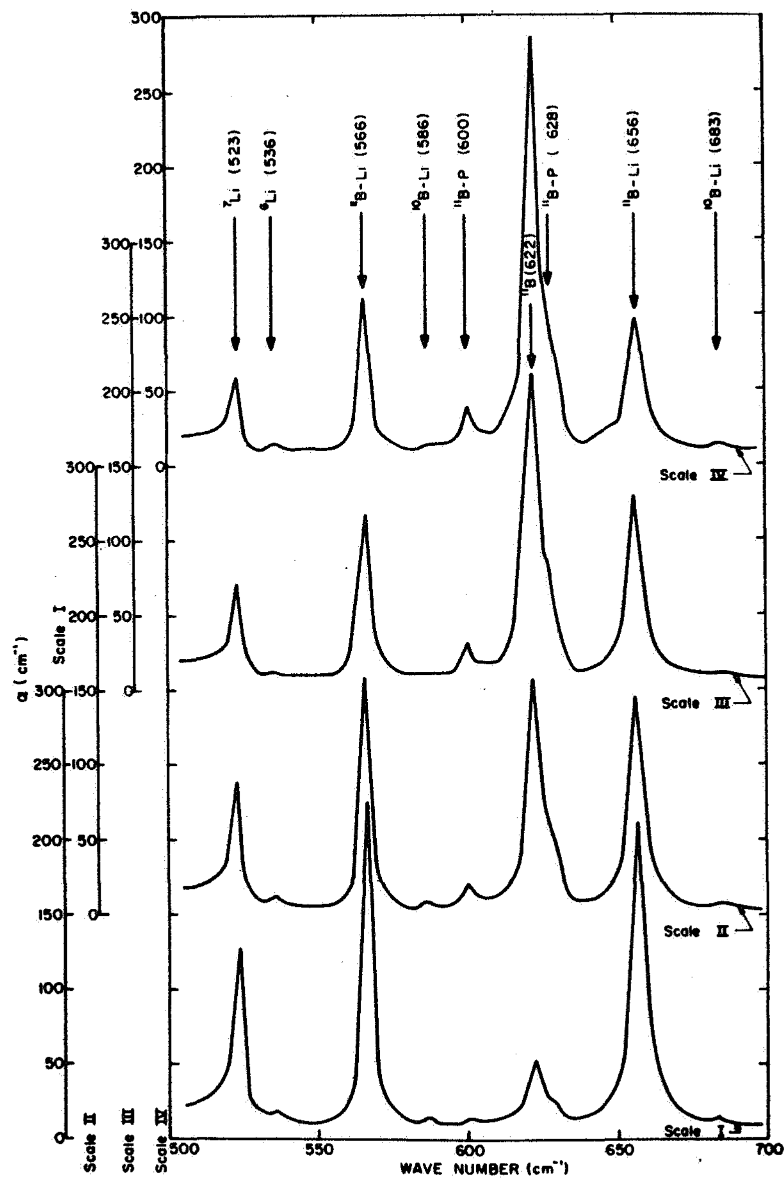

Fig. V-2

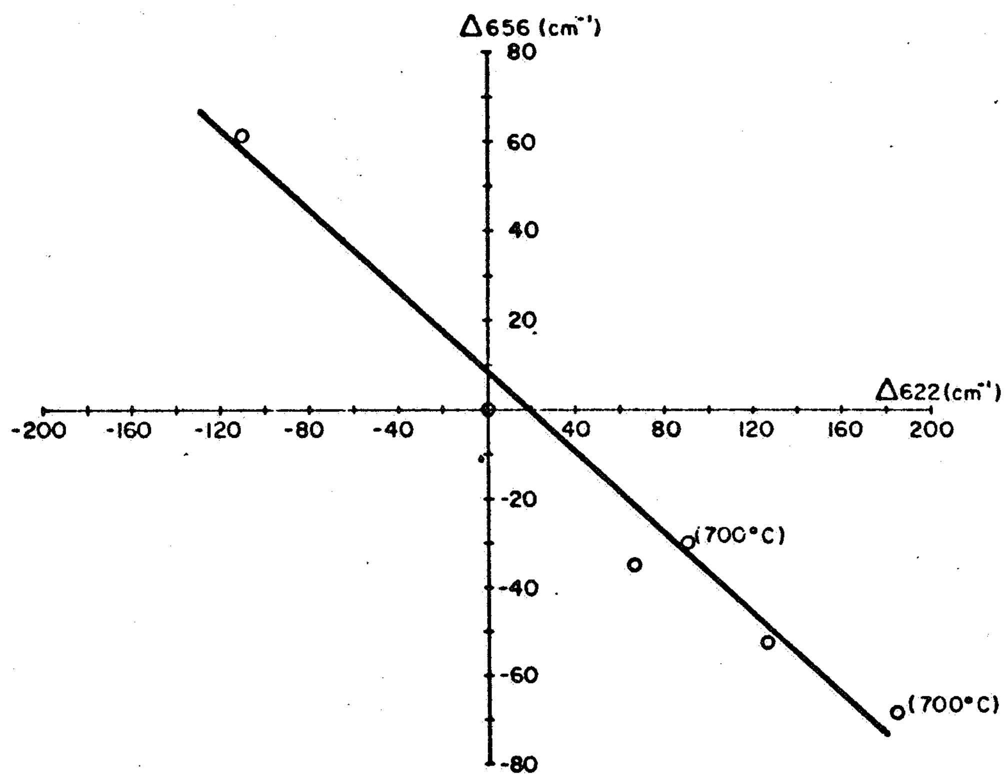

Fig. V − 3

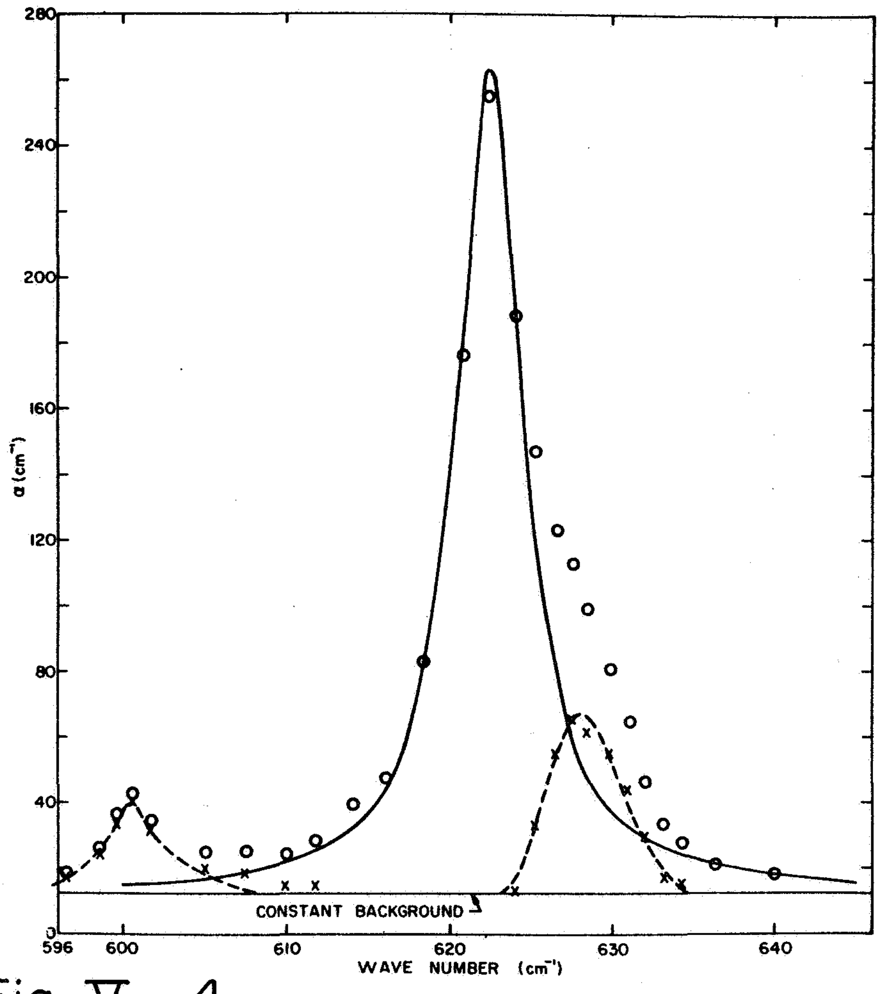

Fig. V - 4

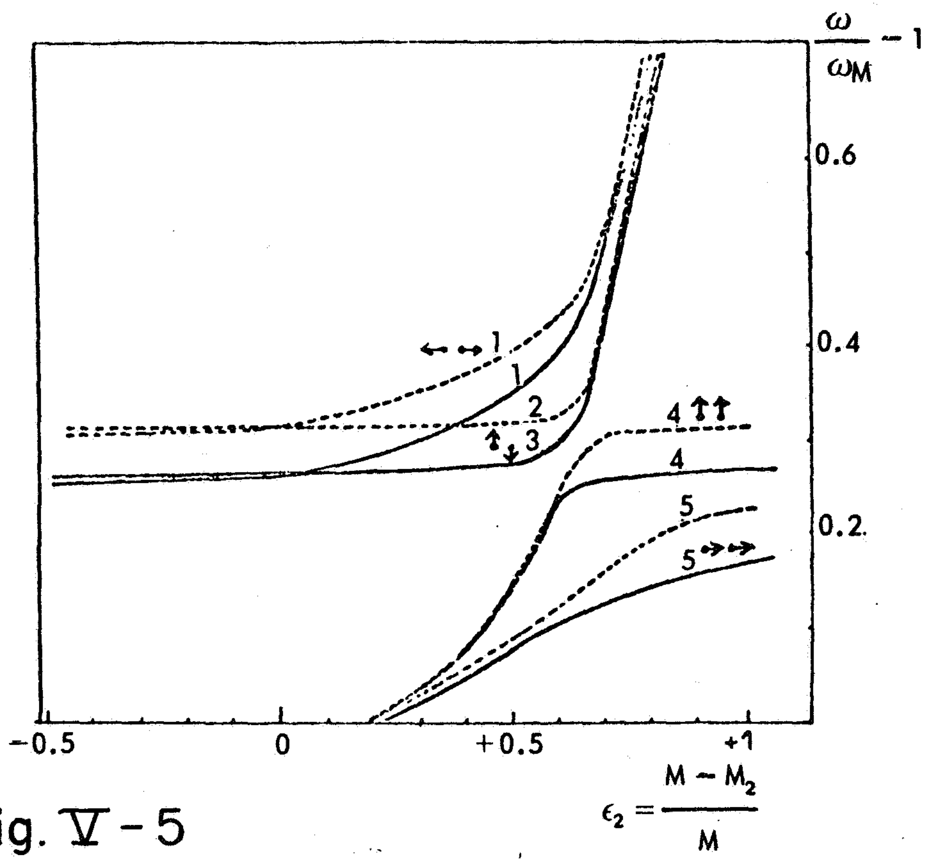

Fig. V - 5